Agriculture, Ecosystems and Environment 306 (2021) 107204

Contents lists available at ScienceDirect

Agriculture, Ecosystems and Environment

journal homepage: www.elsevier.com/locate/agee

Translating the agricultural N surplus hazard into groundwater pollution risk: Implications for effectiveness of mitigation measures in nitrate vulnerable zones

Maria do Rosário Cameira [a,*], João Rolim [a], Fernanda Valente [b], Marta Mesquita [c], Ulrike Dragosits [d], Cláudia M.d.S. Cordovil [b]

[a] LEAF, Instituto Superior de Agronomia, Universidade de Lisboa, 1349-017, Lisboa, Portugal
[b] CEF, Instituto Superior de Agronomia, Universidade de Lisboa, 1349-017, Lisboa, Portugal
[c] CMAFcIO, Instituto Superior de Agronomia, Universidade de Lisboa, 1349-017, Lisboa, Portugal
[d] NERC Centre for Ecology & Hydrology, Edinburgh, UK

ARTICLE INFO

Keywords:
Agri-environmental indicator
Irrigation
Nitrates directive
Nitrogen hazard
Spatialization
Vulnerability
Water surplus

ABSTRACT

In the Nitrate Vulnerable Zones farmers are required to implement measures to reduce the nitrogen (N) surplus. Nevertheless, in some cases the status of the water bodies show that the effect of these measures remains insufficient despite the global decrease in N surpluses. The present work aims to contribute with a method that produces an appropriate indicator for the N mitigation measures effectiveness for reducing groundwater nitrate pollution. The Global Risk Index (GRI) results from overlaying the agricultural N surplus hazard and aquifer vulnerability. It includes both irrigation activity and precipitation contribution to water recharge calculated at the municipality level. It integrates a range of regional datasets combined with monitored nitrate (NO_3^-) concentrations in groundwater under a GIS framework. Results show that the pollution status of the Tagus Vulnerable Zone (TVZ) aquifers has been aggravating in spite of the overall reduction in the N surpluses that resulted from the implementation of the Nitrates Directive measures. Twelve years after the TVZ designation, the GRI indicates high and moderate NO_3- pollution risk, respectively in 33 % and 66 % of the territory. Scenario analysis indicates the potential of targeted measures for ending high risk areas and reducing moderate risk areas to 13 %. This supports that N mitigation measures must be reformulated and spatially targeted according to site specific hazards and vulnerabilities.

1. Introduction

In the Mediterranean region, water is limited in quantity and quality. Climate change may aggravate this problem due to the combined effect of reduced recharge of aquifers, increase in crop water requirements and rising sea levels (Da Cunha et al., 2007; Kilsby et al., 2007; Kovats et al., 2014; Stigter et al., 2014). Hence, the conservation of aquifers as water reservoirs constitutes a major environmental challenge (Arauzo and Bastida, 2015). In this context, nitrogen (N) pollution in water has been a major issue, as it produces negative impacts on human health and biodiversity (Sutton et al., 2011; Erisman et al., 2013).

Diffuse sources of N associated with agricultural activity have been considered the major cause of elevated N in groundwater in the European Union (EU) (Sutton et al., 2011). This is particularly true in Nitrate Vulnerable Zones (NVZs) which are designated as areas of land draining into ground and surface waters vulnerable to pollution from nitrogen compounds from agricultural sources. In the case of groundwater this means nitrate levels exceeding (or likely to exceed) 50 mg L^{-1} (maximum acceptable value, MAV). In the NVZs the continuation of agricultural activities for food production purposes, depends upon the capacity to bring the groundwater quality back to good status.

Mitigation programmes and Directives have been implemented across the EU to reduce nitrogen loads to water bodies. The European Community (EC) Nitrates Directive (ND) (Council Directive 1991/676/EEC) aims to reduce water pollution through nitrates from agricultural sources. The ND requires the Member States to establish Codes of Good Agricultural Practices (CGAP) to be implemented by the farmers on a voluntary basis, and National Action Programs (AP) with mandatory

* Corresponding author.
E-mail address: roscameira@isa.ulisboa.pt (M.R. Cameira).

https://doi.org/10.1016/j.agee.2020.107204
Received 15 April 2020; Received in revised form 2 October 2020; Accepted 6 October 2020
Available online 28 October 2020

measures for the identified vulnerable zones (Cameira et al., 2019). However, reports by EU Member States regarding the status of their water bodies show that the effects of these measures remain insufficient at the European scale (Bouraoui et al., 2011). Thus, it is essential to develop approaches to evaluate the effectiveness of the ND related measures/practices upon the water bodies. Such approaches must also allow the identification of areas with critical sources of diffuse pollution.

Nutrient balances, in particular the gross N balance (GNB) or N surplus, have been used extensively as a proxy for agriculture environmental pressure because of their simplicity at local, regional, and national scales (Bouraoui and Grizzetti, 2011; van Grinsven et al., 2012; Lassaletta et al., 2012; Cameira et al., 2019; Serra et al., 2019). Hansen et al. (2012) found a correlation between N surpluses and nitrate concentrations in groundwater for Denmark. However, large N surpluses do not always coincide with high nutrient losses to the environment (Grizzetti et al., 2008; Baily et al., 2011) particularly in arid climates were recharge rates are low and also when the unsaturated zones are thick (Hagedorn et al., 2018). Thus, the N balance can only indicate the potential hazard. As a next step, this hazard needs to be converted into pressure on the environment and translated into a groundwater pollution risk, by considering the main factors involved in the transport from the bottom of the root zone to the groundwater surface.

The use of experimental methods to quantify actual N losses to the water bodies is limited because routine application of such labour-intensive methods is mostly not viable. Furthermore, measurements are often only made after management decisions have already been taken (i.e., too late). Also, experimental data used for the calculation of N fluxes, e.g. N concentrations in soils, are often not generalizable, due to inter-annual variability in weather patterns, management practices, fertilizer application rates, etc. Alternatively, with more or less complex physically based N transport models, it is possible to quantify N losses for various environmental conditions and management practices (e.g. Cameira et al., 2014; Molina-Herrera et al., 2016; Kasper et al., 2019). Some process-based models can be used in a Geographical Information System (GIS) to predict the temporal and spatial distribution of nitrates in groundwater. It is the case of DAISY-MIKE SHE (Refsgaard et al., 1999), NLEAP-GIS (Li et al., 2020), RZWQM2 (Ahuja et al., 2000), and SWAT (Arnold et al., 2012) models, among others. However, such models require detailed input data, contain many weakly constrained parameters and are often difficult to operate. Furthermore, some models, particularly those to be applied at large river basins are usually set up without including the current management practices (Malagó et al., 2017) which influences considerably N fluxes and storage. Instead, simplified non-process models have been developed for indicative N loss assessment and to identify critical source areas, requiring fewer and more accessible input data (Buczko and Kuchenbuch, 2010). A group of these simplified non-process models is based on assigning ratings to various physical attributes and are called index methods. However, most of them concentrate on groundwater vulnerability assessment rather than on the pollution hazard and groundwater pollution risk. Vulnerability merely indicates whether the characteristics of the subsurface prevent or favour the transport of pollutants into groundwater, without taking into account the actual pollutant loading, which represents the hazard. Thus, these models can indicate high vulnerability but no pollution hazard given the absence of a pollution load. It is the case of SINTACS (Civita and De Maio, 1997) and DRASTIC (Aller et al., 1985; Leone at al., 2009; Kazakis and Voudris, 2015; Meng et al., 2020), among others. Initially this type of models dealt only with groundwater intrinsic vulnerability, which is brought upon by the natural, hydrogeological factors of an aquifer (Vrba and Zoporozec, 1994; van Beynen et al., 2012). Revised versions of the models incorporated few aspects of specific vulnerability (natural parameters and human activities) namely information on land cover (Arauzo, 2017; Salman et al., 2019; Vogelbacher et al., 2019) and performed better than the purely intrinsic methods (Stigter et al., 2006). Nevertheless, there is some doubt that the concept of aquifer vulnerability is a valuable tool for groundwater quality protection, due to discrepancies between nitrate pollution maps and vulnerability maps (Stigter et al., 2006; Foster et al., 2007, 2013; Rizeei et al., 2018). Land cover/use alone does not incorporate information on agricultural practices (e.g. fertilization and irrigation). On the other hand, in addition to groundwater vulnerability, the pollution risk also depends on the existence of a significant pollutant loading, which represents the hazard (Uricchio et al., 2004; Kazakis and Voudris, 2015; Pisciotta et al., 2015). According to Kazakis and Voudouris (2015), the groundwater pollution or pollution risk assessment is achieved by overlaying hazard and vulnerability, which is the concept adopted in the present work.

Table 1
Representative soils in the Tagus Vulnerable Zone (TVZ) and its properties (Cardoso, 1965).

WRB* soil group	Representativeness (% of TVZ area)	Main characteristics
Haplic Podzols	39.9	Sandy loam texture (> 80 % sand); low water retention capacity; high permeability; organic matter < 0.5 %
Fluvisols	17.5	Derived from river or marine sediments deposited regularly; loam texture; moderate water retention capacity; moderate permeability; organic matter [2,5] %
Regosols	11.6	Sandy texture (> 90 % sand); low water retention capacity; high permeability; organic matter [1,3] %
Salic Fluvisols	11.1	Influenced by sea water; silty clay loam texture; high water retention capacity; low to very low permeability; organic matter [1,3] %
Eutric Cambisols	7.4	Sandy loam texture; low water retention capacity; very high permeability; organic matter < 1%
Others	12.5	–

* World Reference Base (Iuss Working Group Wrb, 2015).

The recently completed H2020 Twinning project NitroPortugal coordinated by the University of Lisbon (grant number 692,331) built on the European Nitrogen Assessment report (Sutton et al., 2011), highlighted the need to review current scientific understanding of nitrogen sources and paths specifically for Portugal and wider Mediterranean systems. Recently, Cameira et al. (2019) showed that measures implemented by Portuguese farmers, within the scope of the EC Nitrates Directive and the national Action Plans, have partially succeeded in reducing N surplus at farm level in a designated Vulnerable Zone. One remaining question is how this N surplus reduction impacted on groundwater. Thus, the specific objectives of the study were to: (i) develop an index based methodology for the evaluation of groundwater pollution risk from the agriculture activity (GRI); (ii) assess the global risk of groundwater pollution by nitrates from agricultural activity in a nitrate vulnerable zone and its evolution after the implementation of the EC nitrates directive; (iii) obtain a better understanding of the spatio-temporal distribution of nitrate concentration in the groundwater over a period of 13 years; (iv) discuss the relation between groundwater pollution risk and nitrate pollution status; (v) identify critical areas and predict the global risk under targeted mitigation scenarios.

2. Materials and methods

2.1. Study area characterization

2.1.1. Physical features

Currently Portugal has designated nine Nitrate Vulnerable Zones on the mainland. The Tagus Nitrate Vulnerable Zone (TVZ) is the largest one, representing 60 % of the total designated NVZ area of Portugal. The TVZ is located in the Portuguese part of the river Tagus catchment, which is a transboundary river flowing from Spain to Portugal. The

Table 2
Main characteristics of the aquifers related to the Tagus Vulnerable Zone (Mendonça, 1996; Almeida et al., 2000).

	Semi-confined Aquifer (SCA)		Alluvial Aquifer (AA)
	Right bank	Left bank	unconfined, atmospheric pressure
Total area (km^2)	1629	6875.5	1113.2
Recharge ($hm^3\ y^{-1}$)	150 -200	700	200
(% of precipitation)	15	20	30
Thickness (m)	> 200		< 70
Geology	tertiary formation		quaternary formation
Lithology	limestone formations		sand, silty sands, gravel, sandstones and clays interstratified, overlaying a deposit of sand, gravel and stone
Productivity	median to high		high
Hydraulic properties			
Transmissivity ($m^2\ s^{-1}$)	1.16×10^{-4} to 1.85×10^{-2}		6.9×10^{-5} to 6.7×10^{-2}
Storage coefficient (dim)	2.2×10^{-3}		2.3×10^{-5} to 0.1

climate across the TVZ is Mediterranean (Csa according to the Köppen system) with hot dry summers and mild wet winters. Daily mean and maximum air temperatures over a 30-year period are 13 and 29 °C, respectively. Average annual precipitation for the same period is 697 and 559 mm in the northern and the southern parts of the TVZ, respectively. However, many global climate change scenarios predict an increase in summer temperatures and a reduction in rainfall together with an increase in the risk of summer droughts for the Mediterranean basin (Giorgi and Lionello, 2008; Lassaletta et al., 2012; Kovats et al., 2014; Soares et al., 2017; Cardoso et al., 2019).

About 50 % of the TVZ area has soils with high and very high permeability (Table 1 and Figure S1a in Supplementary Materials). The slope is generally flat, and mild for about 6% of the territory (Fig. S1b).

The study area is part of the Hydrogeological Unit (HU) of the Tejo-Sado Basin. Its Mio-pliocene groundwater system covers an area of about 8000 km^2 and is the most important HU in Portugal (Almeida et al., 2000). The TVZ overlays two main aquifers of this HU. These aquifers, whose main characteristics are presented in Table 2, are: (1) the *Aluviões do Tejo* (hereinafter referred to as Alluvial Aquifer, AA), closer to the soil surface and unconfined at atmospheric pressure, and (2) the *Left and Right banks* (hereinafter referred to as Semi-confined aquifer, SCA) which are tertiary formations, one for each margin of the Tagus (Almeida et al., 2000). Part of the deeper Semi-confined aquifer is located beneath the Alluvial aquifer (Fig. S2). The two aquifers are connected by a leaky confining layer called the aquitard, located at an average depth of 100 m (Mendonça, 2009). Both aquifers are drinking water designated zones.

Mendonça (2009) proposed a conceptual model of flow for the HU (Fig S.2b). The upper Alluvial Aquifer (AA) communicates with the Tagus River through vertical recharge, depending on the hydraulic gradient. The subsurface flow direction is towards the river Tagus and also parallel to the river in the direction of the estuary. The unconfined aquifer is also hydraulically connected to the Tejo and Sado rivers' estuaries and to the Atlantic Ocean, receiving recharge directly from precipitation. The deeper Semi-confined aquifer (SCA) exchanges water with the AA through up or downward leakage through the aquitard. The continued development of pumping rates from this deep aquifer is being balanced by an increase in downward leakage and a reversal in upward leakage.

Recent studies (e.g. Cordovil et al., 2018; Cruz et al., 2019) discuss the status of surface and groundwater quality in the River Tagus watershed, reinforcing the need to develop methodologies to improve its quality and redesign the existing monitoring network.

2.1.2. Economic drivers of the region and main pressures upon the aquifers

The most important economic activity in the TVZ is agriculture which accounts for 63 % of the land use (DGT, 2018). Forests and semi natural areas cover 27 % of the area and urban or artificial surfaces occupy around 4.7 %. In fact, the Utilized Agricultural Area (UAA) is on average 52 % across all municipalities, with a minimum UAA of 5.7 % and a maximum of 83 % (Cameira et al., 2019). Irrigation water comes mainly from groundwater (80 %) by pumping from both aquifers using private drillings and wells (APA, 2016).

The agricultural systems of the region have been intensified during the past decades, especially in the northern and central parts of the TVZ. Currently the most representative crops are irrigated grain maize and horticulture for industrial processing (mainly tomatoes), followed by vineyards, olive groves and permanent pastures (Fig. S3). The overall tendency in the northern part of TVZ during the period 1989–2016 was for an increase of the irrigated area (by 16 %), which is an indicator of agriculture intensification and pressure upon the aquifers. According to Eurostat (2016), livestock production increased in Portugal, and particularly in the TVZ between 2005 and 2016, and consequently the application of manure to the soils.

Table 3 shows the main pressures exerted on the TVZ aquifers, influencing their quantity (water extraction) and quality (N loads), according to the Hydrographic Regions Management Plan produced by the Portuguese Environment Agency (APA, 2016). According to this report, agriculture in general (crop and livestock production) is the activity exerting the highest pressure upon the aquifers, due to the extraction of water for irrigation. The lower aquifer also contributes to urban and industrial water supply to some extent. Regarding the pressure upon water quality, agriculture is also considered the most influent activity. For the AA and the right part of the SCA the major share is attributed to crop production, while for the left SCA the highest pressure is attributed to the livestock production. The same report also concludes that there is a growing need to spatially predict nitrate pollution for a more detailed and perhaps targeted application of the National Action Plan (NAP).

2.2. Data sources

The total period covered by the study ranges from 1989 to 2017 and

Table 3
Main pressures on Tagus Vulnerable Zone aquifers exerted by the different sectors of activity (adapted from APA, 2016).

Aquifer	Pressure on water quantity (%)[a]				Pressure on water quality (%)[b]		
	Agriculture	Industry	Urban	Others	Crop production	Livestock production	Urban
Alluvial (AA)	93.5	3.4	0.6	2.5	58.3	41.6	0.1
Semi-confined (SCA)							
Left bank	60.2	4.5	29.5	5.8	54.0	45.4	0.6
Right bank	72.8	6.3	13.9	7.0	47.3	52.5	0.2

[a] Percentage of the total volume of water abstracted per year.
[b] Percentage of the total amount of N discharged per year.

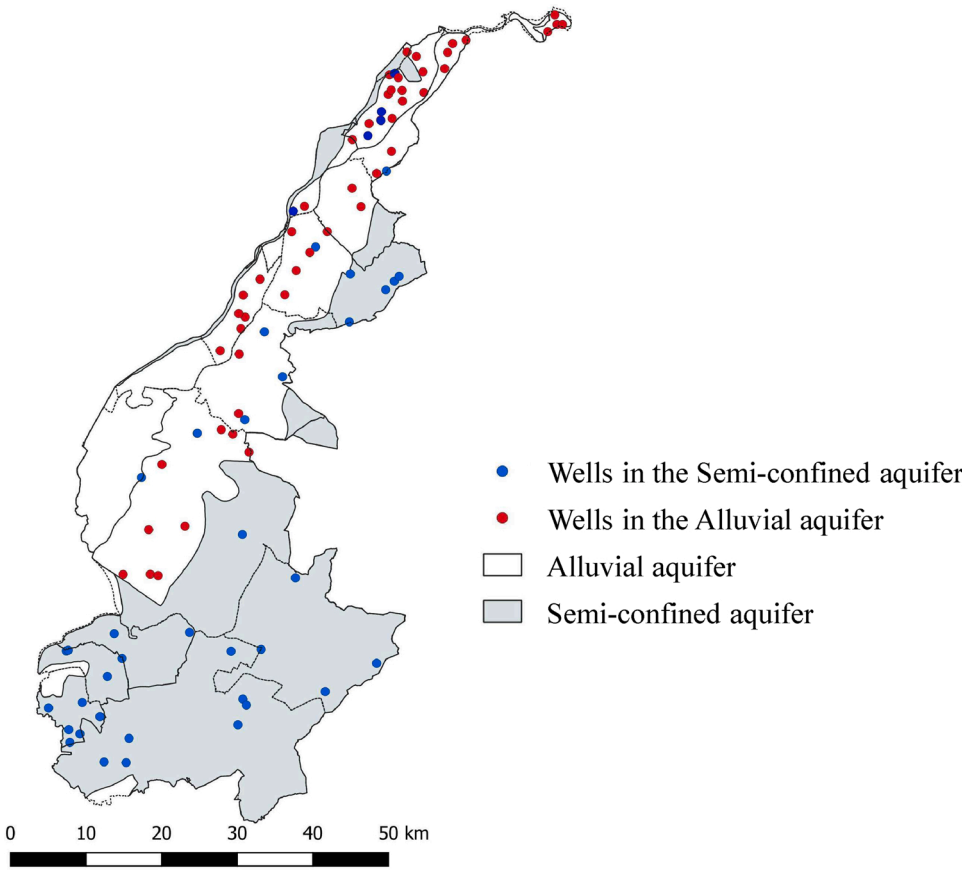

Fig. 1. Ground water quality monitoring stations in the Tagus Vulnerable Zone, part of the national monitoring network.

both soft data (e.g. literature and statistics) and hard data (e.g. time series of nitrates in groundwater) were used.

The geographical data were provided by the Official Administrative Maps of Portugal, CAOP (DGT, 2018). The groundwater quality (measured nitrate concentrations) and quantity (depth of groundwater) data from the national monitoring network was obtained from the National Environmental Water Resources Information System (SNIRH, 2019). The data base presents 96 monitoring stations (wells and drills) for the TVZ, from 2000 to the present (Fig. 1). Data stored in SNIHR are obtained by professionally certified laboratories for water samples collected in the wells of the national monitoring network. In general, two water samples per year are collected in each well, one in early spring and another in early autumn. However, for some wells, only one measurement per year was available, and for shorter periods. Thus, the data analysed in this study refers only to a subset of 80 wells. Meteorological data for the studied period were obtained from a network of meteorological stations covering the TVZ. Different sources had to be used so that the entire studied period and area could be covered (Table S1 and Fig. S4a). Crop and irrigated areas, utilized agriculture area (UAA) and irrigation systems information were collected from the National Statistics Institute website (INE, 2018). Soil types distribution within the TVZ (1: 1 000 000 scale) was obtained from SNIAmb (2019). Topographical data were provided by the Army Map Service. The N surpluses used in the present study to determine the pollution hazard, were previously determined and published by Cameira et al. (2019) for the period 1989–2016. National reports and national and international literature were used to collect data regarding crop water consumptions, crop coefficients, irrigation efficiencies, as it is referred during the document.

2.3. Global risk to groundwater posed by agricultural activity

In the present work, the Global Risk Index model (GRI) was developed to quantify the risk of groundwater pollution with nitrates from agricultural activity. The GRI, which is an index type indicator for nitrates reaching the groundwater, involves a weighted scoring system with several components. The components are indexes that reflect the factors representing the source of N at the soil surface and those influencing the transport of NO_3^- through the vadose zone to the surface of the aquifer (groundwater). Thus, following the concepts presented by Kazakis and Voudouris (2015), the GRI is obtained by overlaying hazard and vulnerability (risk = hazard x vulnerability). The GRI components are: (1) the hazard associated with the gross nitrogen surplus generated by agricultural activity at the soil surface; (2) the water surplus resulting from irrigation and precipitation (specific vulnerability); and the intrinsic vulnerability of the soil/groundwater system related to (3) soil permeability, (4) vadose zone residence time and (5) land topography. The GRI was defined for each municipality of the TVZ as:

$$GRI = I_{NH} \times (\alpha I_{WS} + \beta I_{SP} + \gamma I_{RT} + \delta I_T) \quad (1)$$

where GRI represents the risk of groundwater pollution with nitrates; I_{NH}, I_{WS}, I_{SP}, I_{RT} and I_T are the indexes associated with the hazard (nitrogen surplus), and the vulnerability (water surplus, soil permeability, vadose zone residence time, and topography); α, β, γ and δ are the weights assigned to each vulnerability index.

The GRI classes range from 1 to 5 (Table 4), with the higher values indicating the higher risks of groundwater pollution by agricultural activity. A pollution risk map is then produced, showing the spatial distribution of the pollution risk within the Tagus vulnerable Zone. The calculation of the GRI components is described in the following sections.

Table 4
Classification of the Global Risk Index and the factors contributing for the aquifer pollution risk (the hazard and the specific and intrinsic vulnerabilities).

Global Risk Index-GRI		
Rating	Description	
1	Very Low	
2	Low	
3	Moderate	
4	High	
5	Very high	
N surplus - **Hazard**		
Classes (Kg yr^{-1} ha^{-1})	Description	Rating
[0, 10[	Very Low	1
[10, 25[	Low	2
[25, 50[	Moderate	3
[50, 100[	High	4
[100, 300[	Very high	5
Water Surplus - **Specific vulnerability**		
Classes (mm yr^{-1})	Description	Rating
[0, 50[	Very low	1
[50, 75[	Low	2
[75, 125[	Moderate	3
[125, 200[	High	4
[200, 1000[	Very high	5
Intrinsic vulnerability		
Soil permeability		
Classes (m s^{-1})	Description	Rating
[0, 10^{-7}[	Very Low	1
[10^{-7},10^{-6}[	Low	2
[10^{-6},10^{-5}[	Moderate	3
[10^{-5},10^{-4}[	High	4
[10^{-4}, ∞[	Very High	5
Topography-slope		
Classes (%)	Description	Rating
[10, ∞[	Very Low	1
[5, 10[	Low	2
[2, 5[	Moderate	3
[0.5, 2[	High	4
[0, 0.5[	Very High	5
Vadose zone Residence Time		
Classes (yrs)	Description	Rating
[10, 100[	Very Low	1
[5, 10[	Low	2
[3, 5[	Moderate	3
[1, 3[	High	4
[0, 1[	Very high	5

2.3.1. The agricultural N hazard index, I_{NH}

The N surplus was previously calculated for the TVZ by Cameira et al. (2019) for the period 1989–2016. It corresponds to the amount of N not used by the production system, thus representing a potential threat of pollution. It is the sum of the N losses to the water bodies and to the air and includes N accumulation in soil. Thus, only a part of this surplus will travel to the aquifer, according to the vulnerability (intrinsic and specific) of the studied system. According to the European Environment Agency, N surpluses above 25 Kg N ha^{-1} carry a potential threat for aquifer pollution (EEA, 2018). Although this is a very generic and indicative value which does not take in account the specificity of different catchments, this reference value was used to build the classes of the pollution hazard index shown in Table 4.

2.3.2. Water surplus from irrigation and precipitation index, I_{WS}

Irrigation can be a very important component of the aquifer recharge in Mediterranean areas. Water surplus (WS) is defined in the present work as the excess of water supplied by precipitation and/or irrigation to crops in relation to their water requirements, estimated at a monthly time step in an average 0.5 m root zone. It corresponds to the mass of water flowing through the bottom of the crop root zone during drainage after precipitation and/or irrigation events. It is a relevant factor for this study since leaching occurs mainly due to the convective transport of nitrate. It does not directly correspond to aquifer recharge since it is calculated at the bottom of the root zone and the latter is defined at the groundwater surface, but indicates a potential for NO_3^- transportation. Thus, the WS from irrigation and precipitation is explored in the present work as an indicator of aquifer recharge. Similarly, Arauzo (2017) considered precipitation as a proxy for recharge. WS was determined, for each municipality, for the same periods as the N surplus data (1989–2016). Thus, it reflects the evolution of crop patterns, irrigation technologies and climate variability during the periods before and after the NVZ designation. WS was estimated as a simplified monthly soil water balance (Eq. 2), so that the water surplus from irrigation (spring/summer) and from precipitation (predominantly autumn/-winter) could be identified:

$$WS = P + IRR - ETc - \Delta S \quad (2)$$

where WS is the water surplus, P is the precipitation, IRR is the gross irrigation depth, ETc is the crop evapotranspiration, ΔS is the storage variation in the root zone. All terms are in mm.$month^{-1}$.

The meteorological stations used for the WS calculation are scattered over the TVZ. Therefore, a spatial interpolation of the time series of precipitation (P) and reference evapotranspiration (ETo) was performed. Each municipality's centroid coordinate was extracted using QGIS software (Fig. S4b) and then the spatial interpolation of the climatic data was performed for the 1986–2016 period with the Interpolator software (Rolim et al., 2011) using Inverse Distance Weighting. The spatial distribution of crop areas obtained from statistical data (INE, 2018), was validated by Earth observation images (Rolim et al., 2019). Gross irrigation depths (IRR) were obtained from average measured water consumption data presented in Sousa and Morais (2011) for 2006

Table 5
Average seasonal irrigation depths (IRR) and irrigation efficiencies (EF) for cultivated crop types in the Tagus Vulnerable Zone for 2006 and 2007 (adapted from Sousa and Morais, 2011).

Crop	IRR (mm)	EF (%)
Grain Maize	565	73
Paddy rice	1200	70
Fodder	583	72
Vegetables	500	82
Fruits	787	85
Citrus	800	85
Olive groves	300	88
Vineyards	200	86
Pastures	305	72

Table 6
Range of efficiencies used for each irrigation method/system (adapted from Pereira, 2004).

	Efficiency (%)	
Irrigation method/System	Min	Max
Surface Irrigation		
Traditional	45	70
Modernized	65	85
Paddy rice basins	50	70
Localized		
Drip	70	95
Micro sprinklers	85	95
Sprinkler		
Solid set systems	65	85
Travelling Gun	55	70
Center Pivot	65	85

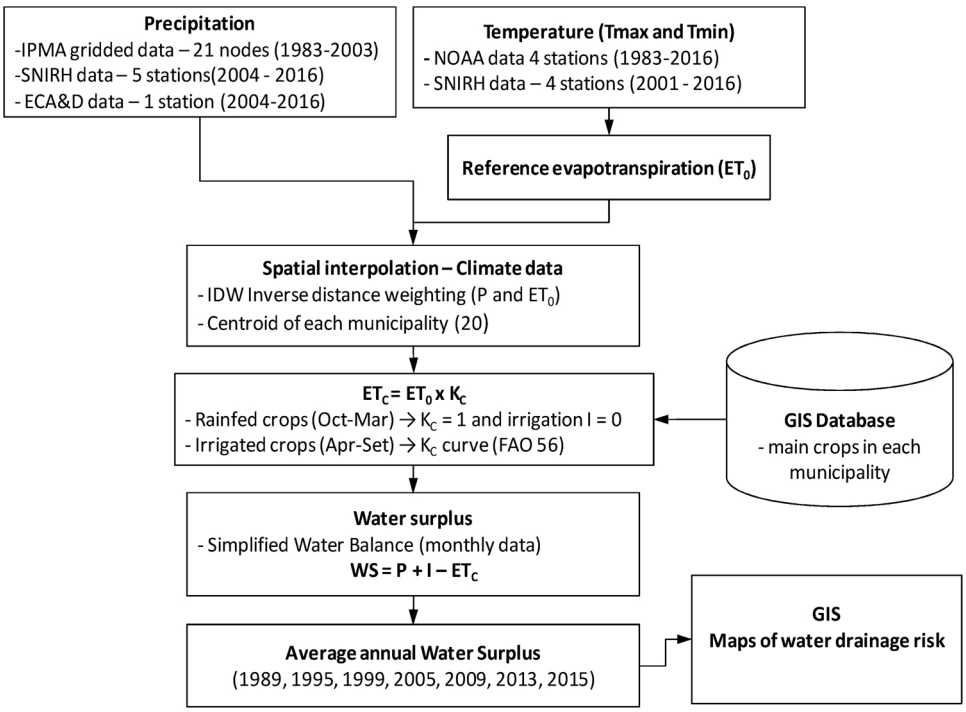

Fig. 2. Flowchart of Water Surplus computations.

and 2007 seasons. These authors collected crop-type specific data directly from farmers, irrigation projects and the farmers' associations (Table 5). To estimate IRR for the studied period, it was necessary to analyse the evolution of the irrigation systems and their efficiencies (EF). Irrigation methods and systems were identified at the municipality level (INE, 2018), by crop type. Thus, an irrigation efficiency was assigned to each crop and year according to the variation intervals presented in Table 6, thereby estimating the irrigation water surplus over the 27 years period.

A summary flowchart of the WS calculation is presented in Fig. 2. The detailed formulation is presented in Appendix A.

Average annual WS was then classified and rated (Table 4) according to its potential impact on groundwater pollution. An average amount up to 50 mm was assumed to be stored in the average root zone, with higher amounts potentially resulting in drainage and/or nitrate leaching, thereby increasing the groundwater pollution risk.

2.3.3. Soil permeability index, I_{SP}

Soil permeability (SP) is another key factor influencing the nitrate transport, particularly in the rootzone. The rating of the permeability classes (Table 4) was based on the soil permeability classes described in USDA (1983) and on the soil data presented in Table 1.

2.3.4. Vadose zone residence time index, I_{RT}

The vadose zone porosity determines the potential for downward movement of the recharge water, impacting the time nitrates need to reach groundwater. The depth of groundwater (GW), i.e. the distance from the soil surface to the surface of the aquifer = thickness of the vadose zone, is an important factor in the global risk analysis, since it determines the distance that NO_3^- need to travel. Based on the GW depths recorded in the monitoring wells, a contour map (raster) was produced by spatial interpolation using the Inverse Distance Weighting method (Fig.S5). The two physical features porosity and depth, were integrated in one index representing the vadose zone residence time. It corresponds to the nitrate travel time from the bottom of the root zone to the surface of the aquifer. Mean residence time, RT (yr) is given by (Keuskamp et al., 2012):

$$RT = \rho_e \frac{D_{GW}}{WS} \quad (3)$$

Where ρ_e is the effective porosity of the vadose zone ($m^3\ m^{-3}$), WS is the water surplus ≈ recharge (m yr^{-1}) and D_{GW} is the groundwater depth (m).

Effective porosity ρ_e, was estimated based upon the lithological class (Table 2) according to Keuskamp et al. (2012) and presents the values of 0.3 and 0.15 $m^3\ m^{-3}$ for the Semi-confined and the Alluvial aquifers, respectively. Average annual residence times were then classified and rated into I_{RT} (Table 4) according with its potential impact on groundwater pollution.

2.3.5. Topography index, I_T

A digital elevation model (DEM) was created based on the contour lines, quoted points and the hydrographic network. Then, a raster map of slopes was generated and classified. Even though the terrain is quite flat, five classes were established considering that the zero slope corresponds to the highest risk (Table 4). Above 10 % slope the associated risk becomes very low since a considerable part of the precipitation/irrigation water flows downhill instead of infiltrating.

2.3.6. Weights associated to each index

According to Pacheco et al. (2015) there are different techniques for factor weighting which may produce markedly different results and hence introduce insecurity in the selection of a technique to properly describe the vulnerability of the studied region. Eq. (1) may be rewritten as

$$GRI = \alpha I_{NH\times WS} + \beta I_{NH\times SP} + \gamma I_{NH\times RT} + \delta I_{NH\times T} \quad (4)$$

where $I_{NH\times WS}$, $I_{NH\times SP}$, $I_{NH\times RT}$, $I_{NH\times T}$ result from combining the hazard index I_{NH} with the vulnerability indexes, I_{WS}, I_{SP}, I_{RT} and I_T, respectively. The values of these new indexes were obtained from a rule-based approach set on expert knowledge (Appendix B, Fig. A1). In the present work, the weights assigned to each index in Eq. (4) were determined by solving a constrained least squares optimization problem (Boyd and Vandenberghe, 2004). The objective function of the quadratic

Table 7
Classification of the observed nitrate concentrations in groundwater for all the monitoring stations during the period 2000-2016.

Nitrate concentration classes (mg L^{-1})	Rating	Description
[0, 10[	1	Very low
[10, 25[	2	Low
[25, 50[	3	Moderate
[50, 75[	4	High
[75, ∞[	5	Very high

programming problem minimizes, for all municipalities and years, the sum of the square differences between the risk of groundwater pollution (GRI) and the index representing the actual groundwater pollution. The latter was obtained by classifying the mean of the observed nitrate concentrations in groundwater for all the monitoring stations, in each municipality and year, according to the criteria presented in Table 7. Based on the conceptual expert knowledge about the system under study, literature (Stigter et al., 2006; Mendes and Ribeiro, 2010) and measured data, the set of constraints $\alpha \geq 0.2$, $\beta \geq 0.1$, $\gamma \geq 0.2$, $0 \leq \delta \leq 0.05$ established the weights' domain. The resulting optimization problem was solved with CPLEX software (IBM, 2017). The final GRI values were obtained by linearly adjusting the result of Eq. (4) to the scale [1,5] dividing by the sum of the four weights.

Modelling was performed using data from 2000–2017 and then used to predict the groundwater pollution risk since 1989. The performance of the proposed index was assessed by a visual analysis between maps of the GRI index and observed nitrate concentration.

2.4. Statistical methods for nitrates in groundwater analysis

2.4.1. Gridding of nitrate concentrations

To produce a contour map of the spatial distribution of NO_3^-, the nitrate concentrations measured in the monitoring wells were interpolated using Inverse Distance Weighting in Surfer 10 (Golden Software, 2011).

2.4.2. Nitrate trend analysis

Nonparametric techniques were used to detect monotonic trends in the longitudinal data of NO_3^- concentrations in groundwater. Bartels' rank test of randomness (Bartels, 1982) was applied to analyse the significance of a trend in a sequence of observations. Following Bartels (1982) procedure, the exact p-value of the test was calculated for small samples (with 10 or less values) while a beta approximation of the randomize distribution was used for larger ones. Whenever a significant trend was detected, Spearman's rho (ρ, rank correlation coefficient) and the coefficients of the trend line were calculated: the slope (b) was estimated by Theil–Sen's method (Thiel, 1950; Sen, 1968) and the intercept by the estimator proposed by Hettmansperger et al. (1997). These analyses were done in R (R Core and Team, 2018) with the RStudio software (R Studio Team, 2018) using the packages 'randtests' (Mateus and Caeiro, 2014) and 'mblm' (Komsta, 2019).

2.5. Spatially targeted mitigation scenario analysis

Based upon the maps showing the spatial distribution of the pollution risk within the Tagus Vulnerable Zone, and according to the relative importance of hazard (magnitude and N sources) and vulnerability in the different municipalities, the optimized GRI model was used to estimate the impact of spatially targeted measures. Risk maps were produced and compared to the baseline situation which corresponds to the year 2016.

3. Results and discussion

3.1. N surplus hazard

Fig. 3 shows the spatial distribution of the N hazard index (I_{NH}), classified from "very low" (1) to "very high" (5). In the early study period, the hazard was very high (> 100 kg ha^{-1} yr^{-1}) across most of the TVZ, reducing substantially over time, especially in the northern part where the irrigated crops are the main agricultural activity. In these areas the hazard is classified as moderate (25 < N surplus < 50 kg ha^{-1} yr^{-1}) in 2016. This decreasing trend is partly associated with the NVZ designation of the territory which occurred gradually between 2004 and 2010, and the compulsory mitigation measures. According to Cameira et al. (2019), the reduction of mineral and organic fertilizers effectively reduced the N surplus in the northern part of the TVZ. Before 2004, other factors, including EU policies such as the Common Agricultural Policy and increased mineral fertilizer costs were responsible for the N surplus decrease. In the central region (municipality 7) the hazard did not change substantially during the entire period. In most of the TVZ regions the N surplus is due either to high fertilization of intensive crops, or to the production of big amounts of livestock manure, while in the central area these two inputs contribute simultaneously. Thus, even though the mitigation measures cause a decrease in the N surplus absolute values, it is not enough to decrease the hazard class. On the other hand, in the southern region, the N hazard has decreased, although still classified as a "high hazard" (50 < N surplus < 100 kg ha^{-1} yr^{-1}) during the recent past. This is likely associated with the high livestock production in these southern municipalities, resulting in large amounts of manure spread on the cultivated land.

3.2. Water surplus/aquifer recharge specific vulnerability

Water surplus was calculated from the water balance performed at the municipality scale (Eq. 2) considering precipitation and irrigation as inputs and crop water requirements as outputs. The average crop coefficients (Kc) for the mid-season crop stage (Fig.S6) were used to calculate the crop water requirements and present values ranging from 0.74 to 1.20 among municipalities. The differences are associated with the heterogeneous crop distribution over the TVZ. The lower Kc values refer to a high percentage of orchards and olive groves (e.g. municipality 16), while the higher Kc values are associated with the predominance of maize (e.g. municipality 12). In some municipalities the average Kc values changed substantially during the studied years. In municipality 1, horticultural crops were gradually replaced by paddy rice, resulting in the increase of Kc values. An opposite trend is observed in municipality 20, where the increasing area of vineyards and pastures explain the reduction in average Kc. Most crop water demands are met with irrigation, primarily from April to September, when evapotranspiration pays an important role in the water balance.

Fig. 4 shows the evolution of the TVZ overall water surplus as well as the WS for each municipality. The lower WS calculated for the second period, as compared with the adjacent periods, is associated to a prolonged drought occurring from 1991 to 1995 (Pires et al., 2018). An overall decreasing trend is observed, possibly associated with: (1) the increase in irrigation efficiency, reflecting the technological evolution of irrigation systems, from traditional surface irrigation to pressurized systems e.g. centre pivots and drip irrigation systems; (2) the decrease in the annual precipitation values following the climate change trends already observed in Portugal (Shahidian et al., 2014; Pires et al., 2018).

Fig. 3 shows the maps of the water surplus index, used in the present work as a proxy for the recharge. In 1989, the water surplus vulnerability was very high (> 200 mm yr^{-1}) over the entire TVZ, likely due to the very low efficiencies of the traditional surface irrigation methods used in high water demanding crops such as rice, vegetables and maize. In average, 50 % of the applied water was lost by percolation below the root zone, which together with the autumn/precipitations induced a

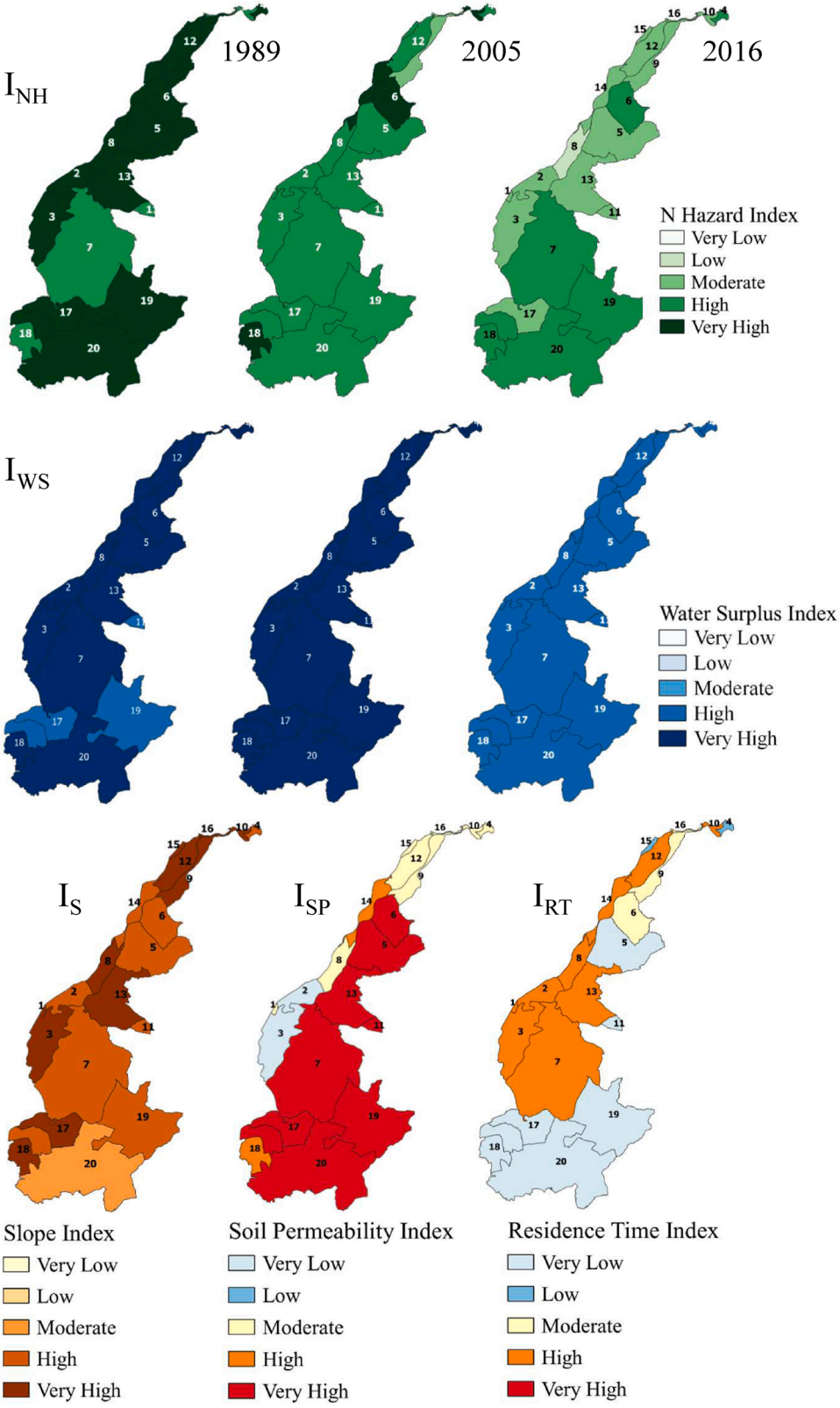

Fig. 3. Spatial distribution of the nitrogen hazard index (I_{NH}), and the water surplus (I_{WS}), slope (I_S), soil permeability (I_{SP}) and residence time (I_{RT}) vulnerability indexes. Evolution in the Tagus Vulnerable Zone to nitrates.

considerable recharge of the aquifer and consequent efficient transport of the N surplus. In spite of the modernization of the irrigation systems from 2000 onwards, with efficiencies of 80 and 95 % for sprinkler moving systems and drip systems, respectively, the water surplus vulnerability index remained high (125−200 mm yr^{-1}). This can be attributed to the heavy precipitations occurring during autumn/winter season when the crop uptake is very low, as is typical for Mediterranean climates. Fig. 5 shows that during the irrigation season (April to

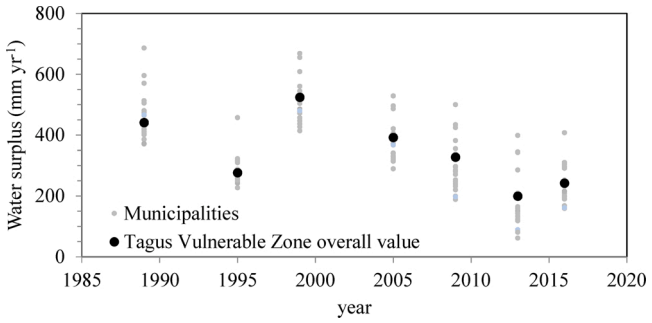

Fig. 4. Evolution of the annual water surplus in the Tagus Vulnerable Zone, by municipality and overall value for the territory.

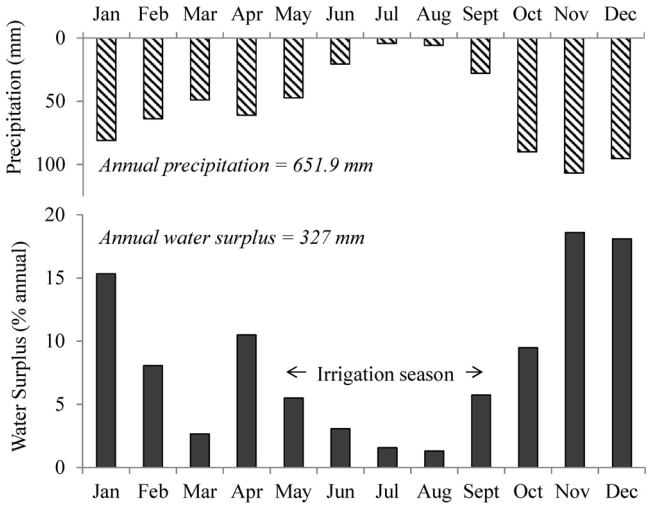

Fig. 5. Monthly distribution of the average Water Surplus and 30 years' average monthly precipitations.

September) when there is almost no precipitation, the recharge associated vulnerability can be minimized through the proper management of the irrigation systems. However, this vulnerability will stay high during autumn/winter due to precipitation. Thus, after the spring crops harvest in September/October, there is always a moderate to high potential for N surplus stored in the rootzone to be transported by the percolating water.

3.3. Intrinsic vulnerability

Due to the flat and mild slopes that characterize the TVZ the majority of water from precipitation and irrigation that reach the soil surface infiltrates, justifying the moderate to very high slope vulnerability indexes (I_S) presented in Fig. 3. Furthermore, the majority of the TVZ territory presents high vulnerability indexes associated with soil permeability (I_{SP}) (Haplic Podzols and Regosols in Figure S1a with permeability > 200 cm day^{-1}). The Thionic Fluvisols and the Fluvisols located in a strip of land parallel to the river Tagus, are responsible for the low and the moderate vulnerability indexes. Conversely, Fig. 3 shows that the vulnerability index associated with the residence time (I_{RT}) in the vadose zone is lower in the southern TVZ, where the Semi-confined aquifer located at depths > 15 m (Fig. S5b). This vulnerability is higher in a strip parallel to the river Tagus, where the Alluvial aquifer is close to the soil surface (Fig. S5). The RT associated vulnerability (Fig. 3) varies from very low (> 10 years) mainly in the southern part to very high (0–1 year) in a strip parallel to the river Tagus. This gives distinct vulnerabilities to the different regions of the TVZ.

3.4. Global risk index

The groundwater pollution risk index was obtained by a sequential method that used a rule-based approach to combine the N surplus hazard with the vulnerability factors, followed by a weights' optimization routine. This sequential method is an alternative approach to other empirical predictive models such as machine-learning methods (e.g. Rodriguez-Galiano et al., 2014; Nolan et al., 2014, 2015) or multiple linear regressions (e.g. Boy-Roura et al., 2013). Like machine-learning

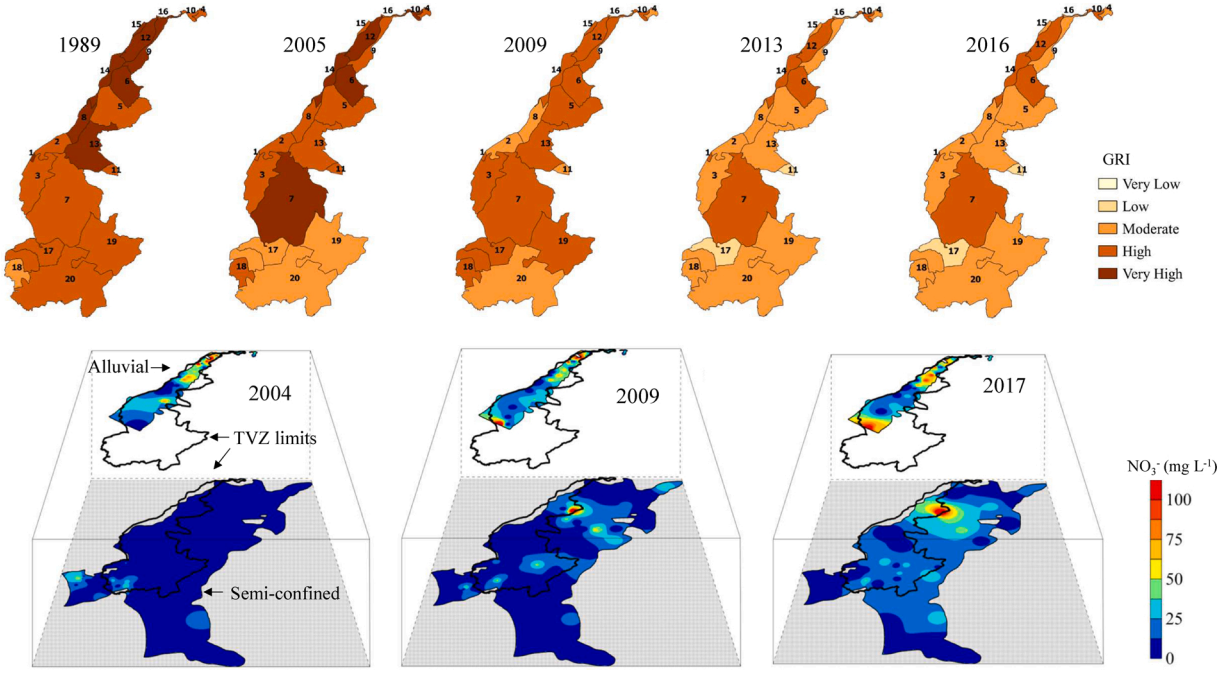

Fig. 6. Top graphs: Spatial distribution and evolution of the global risk for groundwater contamination with nitrates from the agricultural activity (GRI), for the Tagus Vulnerable Zone; Bottom graphs: Nitrate concentration maps for the overlaying Alluvial aquifer and Semi-confined aquifer in the Tagus Vulnerable Zone. The limits of the TVZ are projected over the two aquifers for better orientation.

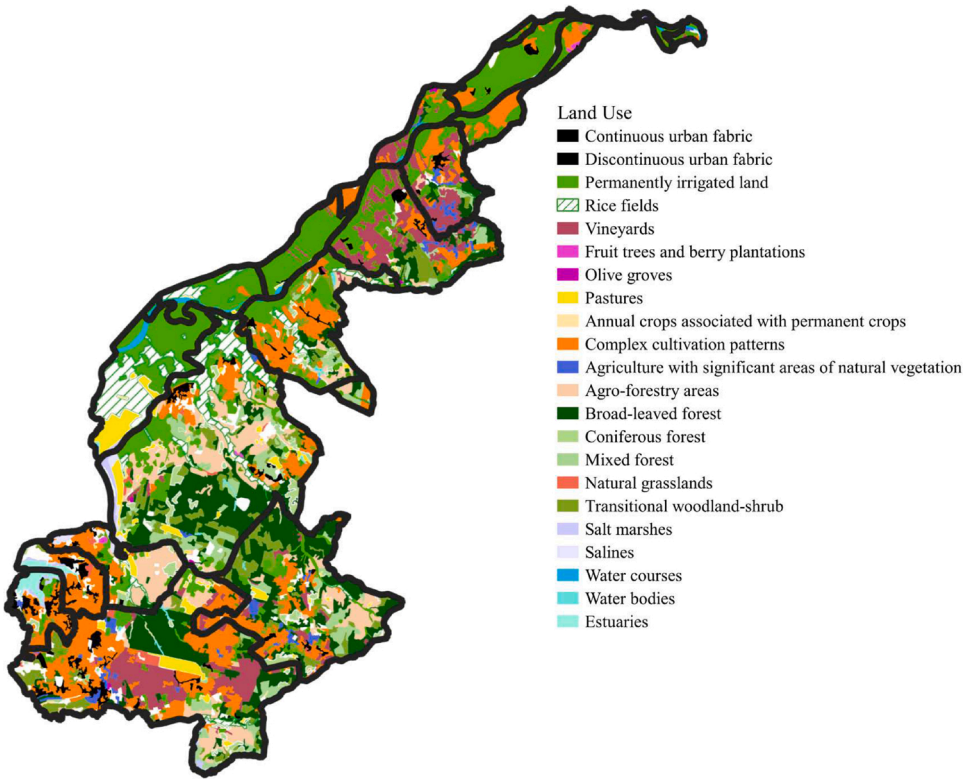

Fig. 7. Land cover in the Tagus Vulnerable Zone, adapted from CLC (2018).

methods, index models are non-parametric techniques that do not required any statistical distribution assumptions. Although machine-learning methods can handle large datasets, with many input variables, they are fully computational algorithms that do not take advantage of human expertise. Being defined on a small number of variables, the GRI model may take advantage of human knowledge to achieve a better description of the system under study. The use of a rule-base scheme gives some flexibility when combining the hazard with the vulnerability indexes. For example, the pollution risk associated with a high value of I_{NH} and a low value of I_{WS} is different from the risk assigned to a low I_{NH} and a high I_{WS}. Additionally, the GRI index model does not require a large amount of data to be implemented and it is very easy to apply.

The overlay of the hazard layer and the vulnerability layers described above result in a Global Risk Index for groundwater pollution posed by agricultural activity (GRI) (Eqs. 4). The risks associated to the water surplus (I_{NHxWS}), soil permeability (I_{HNxSP}), vadose zone residence time (I_{NHxRT}) and slope (I_{NHxS}) present the weights $\alpha = 0.2$, $\beta = 0.1$, $\gamma = 0.39$ and $\delta = 0$, respectively, obtained from the least squares' optimization problem. The highest weight was assigned to the vadose zone residence time. RT depends upon the conductive properties as well as with the depth of the groundwater, which have a higher impact on nitrate enrichment in groundwater than the other vulnerability components. As in similar studies (Stigter et al., 2006; Mendes and Ribeiro, 2010), smaller weights were assigned to recharge and soil permeability. For the present conditions, the slope did not influence the GRI. The spatial distribution of the GRI (Fig. 6 – Top graphs) illustrates how, before the implementation of the ND (1999), almost all of the territory presented very high (34 %) or high (56 %) risk for groundwater pollution. In the northern part the very high risk is mainly due to the high hazard index (Fig. 3). In 2005, the GRI decreased, following the trend of the N hazard index discussed previously, with the exception of municipality 12, where in spite of the decrease in I_{NH} from very high to high, the GRI remained very high. In the southern part, there is a moderate risk of groundwater pollution by the agricultural activity. In 2016, twelve years after the first designation of the Tagus Vulnerable Zone, none of the municipalities have a very high risk, but 38 % of the area still presents a high risk, in spite of the moderate hazard. In the southern part the risk has stabilized during this period, with the exception of one municipality presenting a low risk (19 % of the area). Fig. 3 shows that the N hazard has also stabilized in this area.

In the land strip parallel to the river Tagus, the high vulnerability associated to very low residence times (0.4–2 years) is responsible for high pollution risks, even in those cases where the hazard risk has decreased to moderate after the implementation of the ND/AP related mitigation measures (Appendix C). In the southern part, the GRI is high, in spite of the very low vulnerability associated to nitrate residence time due to the higher depths of the Semi-confined aquifer (Fig. S5). Nevertheless, in these areas, the N hazard is still high 12 years after the TVZ designation.

The distinct behaviour among regions within the TVZ is also associated to the landcover (Fig. 7). The areas along the river are mainly cultivated with permanently irrigated crops which require very high inputs of water and N. On the other hand, in the central and southern

Table 8
Summary of nitrate concentrations in the aquifers of the Tagus Vulnerable Zone for the period 2000 to 2017.

Aquifer	wells	years with data	data points	$[NO_3^-]$ (mg L^{-1})				CV
				Min	Median	Average	Max	(%)
Alluvial	44	18	905	0.2	20.7	36.9	221.8	112
Semi-confined	36	18	694	0.2	3.0	13.0	200.0	196

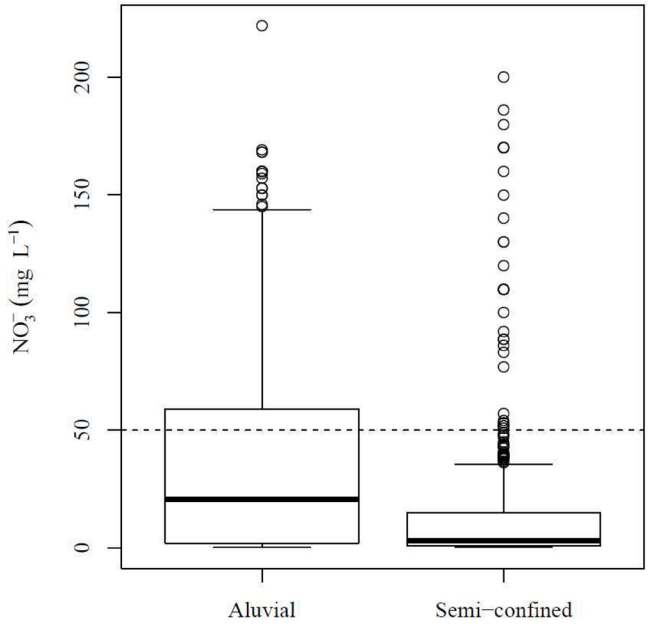

Fig. 8. Box plots for the nitrate concentrations in the alluvial and the semi-confined aquifers in the Tagus Vulnerable Zone, from 2000 to 2017.

Table 9
Summary of nitrate concentrations in the aquifers of the Tagus Vulnerable Zone for the period 2000 to 2017 by sampling semester.

Season	data points	$[NO_3^-]$ mg L^{-1} Min	Median	Max	CV (%)
Alluvial aquifer					
Semester I (February/March)	470	0.2	20.0	169.0	112
Semester II (September/ October)	435	0.2	21.0	221.8	113
Semi-confined aquifer					
Semester I (February/March)	366	0.2	3.2	200.0	197
Semester II (September/ October)	328	0.2	2.8	170.0	192

part the land is mainly occupied by agroforestry, vineyards and complex cultivation patterns, the latter associated to family-based agriculture. However, as shown by Cameira et al. (2019), the high N surpluses in these areas are associated with large amounts of manure that are produced by livestock (the main agriculture activity) and applied to the fields.

3.5. Nitrate concentrations in groundwater

3.5.1. General analysis and trends in groundwater

Table 8 shows the results of the statistical analysis of nitrate concentrations at the 80 monitoring wells in the TVZ retained in this study. Nitrate has been found in the upper (Alluvial) and lower (Semi-confined) aquifers with similar maximum concentrations of 222 and 200 mg L^{-1}, respectively. The average and median concentrations are, however, 2.6 and 6.9 times smaller in the lower aquifer, respectively. The variability is high for both aquifers, reflecting a large heterogeneity in both time and space. Furthermore, there is a large number of outliers in the Semi-confined aquifer (Fig. 8) highlighting this considerable variability which likely indicates the presence of pollution hot spots.

A statistical summary of the NO_3^- concentration data by season is presented in Table 9. For the upper Alluvial aquifer, the maximum concentration was measured in the second semester, early fall, at the end

Table 10
Percentage of wells with maximum values of nitrate concentrations by class for the period 2000 to 2017.

Aquifer	% wells with max $[NO_3^-]$ in the range 0 – 50	50–100	> 100
Alluvial	45.5	22.7	31.8
Semi-confined	86.1	8.3	5.6

Table 11
Monitoring wells with significant trends of nitrate concentrations ($p < 0.05$). Total number of wells per aquifer and correspondent percentage by class of maximum $[NO_3^{-1}]$.

Trend	Number of wells	Class of maximum $[NO_3^{-1}]$ (mg L^{-1}) 0–50	50–100	>100
Alluvial				
Decrease	9	45	22	33
Increase	9	78	11	11
No trend	26	35	27	38
Semi-confined				
Decrease	5	100	0	0
Increase	16	94	6	0
No trend	15	74	13	13

of the spring/summer irrigated season. This is likely due to the Alluvial aquifer being close to the soil surface (1–14 meters), and therefore responding fast to agricultural activities (irrigation and fertilization) in summer and to the heavy precipitation characteristic in Mediterranean regions in winter. In fact, during winter aquifer recharge from precipitation can contribute to the dilution of the groundwater, decreasing nitrate concentrations. Other authors, e.g. Rotiroti et al. (2019), describe this positive dilution effect as a result of high groundwater recharges with low nitrate concentrations. In the Semi-confined aquifer, maximum concentrations were measured in the first semester, early spring. During the autumn/winter season the water surplus is higher (Fig. 5). Thus, any nitrate applied during a spring/summer season and not used by the crops is gradually transported through the thick vadose zone or through the aquitard (according with the location) and may reach the deeper aquifer next spring, with a considerable time-lag. Nevertheless, in spite of this tendency with a reasonable conceptual explanation, no statistically significant differences were found between semesters, which in part is due to the high variability of the concentrations.

Table 10 shows that in the Alluvial aquifer, maximum nitrate concentrations corresponding to the MAV of 50 mg L^{-1} are exceeded at 55 % of the monitoring sites while maximum concentrations of 100 mg L^{-1} are exceeded at 32 %. For the deeper aquifer, 86 % of the monitoring wells show nitrate concentrations lower than 50 mg L^{-1} and only 6% show values higher than 100 mg L^{-1}. Other studies report higher nitrate concentrations in Alluvial aquifers (e.g., Brindha and Elango, 2013). This is usually attributed to shallow ground water being more vulnerable to diffuse pollution from agriculture due to shorter travel times, as also shown in the present work.

Table 11 shows the results of the trend analysis of the time series of nitrate concentrations in groundwater, per well. Overall, 39 wells (49 %) show significant trends in the nitrate concentrations, 14 of which (36 %) have decreasing trends. For the remaining 25 wells with significant trends, nitrate concentrations are still rising significantly, with rates varying from 0.013 to 3.6 mg L^{-1} yr^{-1} in the Alluvial aquifer and from 0.017 to 2.0 mg L^{-1} yr^{-1} in the Semi-confined. The results by aquifer show that in the Alluvial the same number of wells show increasing and decreasing trends, with the majority still in the “safe zone” below the MAV of 50 mg L^{-1}. However, 11 % of the wells show concentrations higher that 100 mg L^{-1} and still rising. The analysis of the temporal trend for each well revealed that although some wells in the upper

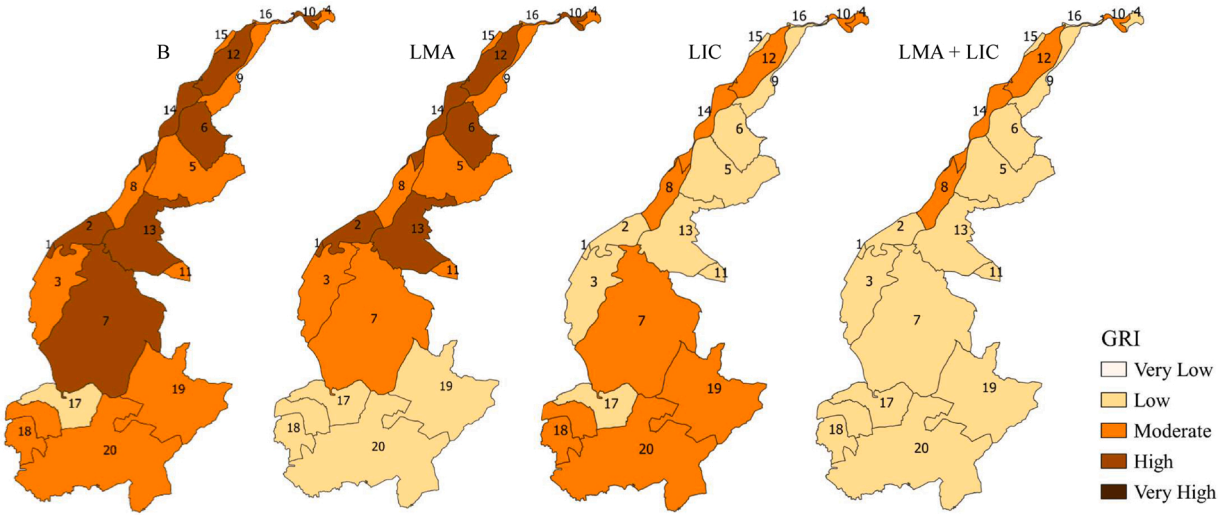

Fig. 9. Global Risk Index for the baseline and the targeted mitigation scenarios: B – baseline (2016), LMA - low manure application, LIC – low-input demanding crops, LMA + LIN – both scenarios simultaneously.

Alluvial aquifer show strong decreasing trends with rates as high as 4.2 mg L^{-1} yr^{-1} (Fig. S7a), some still show concentrations exceeding 100 mg L^{-1}. Besides, a couple of wells with current concentrations above the MAV show increasing trends above 2.9 mg L^{-1} yr^{-1}. There are also several wells with concentrations much higher than MAV that show no trends indicating that high pollution levels will continue if no additional measures are implemented.

For the Semi-confined aquifer (Table 11, Fig. S7b), almost all the wells with increase trends still show very low concentrations, which may indicate that the pollution of the Semi-confined aquifer is starting. In the southern part of the TVZ there are municipalities (17 and 20) where some wells show strong increasing trends (but still bellow MAV) while other municipalities (18, 19, 20) present decreasing trends. Like in the upper aquifer, there are two wells with concentrations above the MAV that show no trends.

3.5.2. *Spatial analysis of the groundwater NO_3^- concentrations: pollution maps*

As described in Sections 2.1.1 and Figure S2 (Supplementary Material), the TVZ aquifers are partially overlaid, with a semi permeable layer between them (an aquitard). However, in Fig. 6 (bottom graphs) the aquifers are presented overlaid but separated to facilitate analysis of their pollution status for 2004 (year of the first NVZ designation), 2009 (after the last designation), and 2017 (most recent available data). A large spatial variability of [NO_3^-] in groundwater can be observed, with the northern and central parts more severely polluted than the southern part. Also, the upper Alluvial aquifer is more severely polluted than the lower Semi-confined aquifer. In 2004 the monitoring wells of the Alluvial with [NO_3^-] > 50 mg L^{-1} were concentrated in the northern part of the TVZ. In 2009 the pattern is similar, but a hotspot emerged further south (municipality 7) and increased in area by 2017. The problem persists in the northern region of the TVZ across the study period. The strong gradients from the early period have been decreasing during the years, but in the form of spreading of the groundwater pollution, instead of much improvement. During the study period the area of the Alluvial aquifer showing concentrations higher than 50 mg NO_3^- L^{-1} has increased by 122 %. Regarding the lower Semi-confined aquifer, although in 2004 nitrate concentrations were below the recommended maximum value of 25 mg L^{-1}, a pollution hotspot (> 50 mg L^{-1}) appeared in 2009 (beneath municipalities 5 and 6) and has persisted to the present day. During the study period, the area with concentrations between 25 and 50 increased from 0 to 28 %. These areas are directly underneath the most contaminated areas in the Alluvial aquifer in the northern part of the TVZ. The lag existing between these two occurrences is probably related with the higher groundwater depth of the Semi-confined aquifer in relation to the upper aquifer (Fig. S5), the superposition of both aquifers and the aquitard between them (Fig. S2a).

In summary it seems that, even with the compulsory measures imposed by the EC and the National Action Plan, the nitrate pollution in the lower aquifer is aggravating rather than improving, as high concentrations slowly infiltrate previously clean groundwater.

3.6. *Relation between the global risk index and the nitrates in groundwater*

In most cases there is a reasonable correspondence between the estimated groundwater pollution risk with nitrates from agriculture activity using the GRI model and the actual groundwater pollution (Fig. 6), in particular for the Alluvial aquifer. The GRI was capable of explaining why in the areas were in the recent years the N surplus has decreased significantly to a moderate and low hazard (Fig.3), the nitrate enrichment in groundwater has been aggravating. It is the case of the northern part of the Alluvial aquifer, where the decrease of the global risk has been limited by the moderate and high vulnerabilities associated to the soil permeability and the nitrate residence time in the vadose zone, respectively (Fig. 3). These results are in line with other studies (e.g. Lord et al., 2002; Sieling and Kage, 2006; de Ruijter et al., 2007; Grizzetti et al., 2008; Baily et al., 2011) stating that it is unclear if the N balance (or N surplus) is capable of reflecting actual nitrate leaching. However, the present study shows that even though the N surplus is not the most appropriate agri-environmental indicator for this type of studies, its calculation is fundamental since it constitutes the N loading hazard and incorporates the effects of agricultural practices and their change over time. It can be seen also in Fig. 6 (bottom graphs) that in the northern TVZ territory, in 2009, nitrates crossed the aquitard beneath the Alluvial and are reaching the Semi-confined aquifer, with an aggravating situation until 2017. In the southern part, a lighter blue (more polluted) area started to appear in the Semi-confined aquifer, and are slowly developing as exemplified in Fig. 9b, in several wells of municipalities 17 and 20. In this case, the vulnerability associated to the very high soil permeability is the limiting factor for achieving a low rated GRI.

The GRI estimation methodology includes the nitrate resident time in the vadose zone, thus indirectly contemplates the thickness and porosity of the vadose zone. The estimated transport times suggest that any change in the N loading hazard by the application of the ND/AP

mitigation measures, will take from 0.4–7 years to be reflected in the Alluvial aquifer, while for the Semi-confined aquifer it will take up to 56 years. Nevertheless, some discrepancies are observed between the GRI index and the actual groundwater pollution, in particular for the Semi-confined aquifer. Some possible explanations are discussed next.

The actual nitrate residence time in the vadose zone can be higher due to a significant amount being retained and stored. This, increases the lag between any changes in the agricultural practices to reduce nitrogen loading at the soil surface and its impacts on groundwater quality (Baily et al., 2011; Wang et al., 2015; Ascott et al., 2017; Kim et al., 2019). Furthermore, in the areas where the Semi-confined aquifer in overlaid by the Alluvial, the aquitard will considerably slow down the convective transport of nitrate due to its low hydraulic conductivity, which is not being accounted for in our empirical model.

Nitrate is commonly thought to be conservative in groundwater and retardation is also negligible for the majority of soils. Nevertheless, some mass attenuation can occur especially due to denitrification and is likely to occur when the travel times are long, which is the case of the Semi-confined aquifer. This biogeochemical process is extensively addressed by Rivett et al. (2008).

The advective transport within the saturated zone and the transport by subsurface horizontal flow within the vadose zone can also be responsible for the mismatch, as found elsewhere by Holman et al. (2005); Stigter et al. (2006); Debernardi et al. (2008); Arauzo and Martínez-Bastida (2015). As described in Section 2.1.1, there is a subsurface flow in the Alluvial aquifer towards the river Tagus and also parallel to the river in the direction of the estuary (Mendonça, 2009). Also, in the Semi-confined aquifer, there is a strong hydraulic gradient towards Tejo and Sado rivers' estuaries. Thus, groundwater flows from outside into the TVZ area, which can increase/reduce nitrate concentrations through mixing with water of a higher/lower concentration due to accumulation/dilution processes (Arauzo et al., 2011; Martínez-Bastida et al., 2010; Stigter et al., 2006). As stated by Arauzo and Valladolid (2013) and Arauzo (2017), the areas through which a soluble pollutant like nitrate enters the vadose zone may not necessarily coincide with the affected areas of the receiving aquifer, i.e. the correct area to be designated as vulnerable zone may not coincide with the contaminated areas of the aquifer beneath. Therefore, the delimitation of the vulnerable zone may need to be adjusted according with the subsurface and groundwater flows within the watershed instead of following administrative boundaries as it is now.

3.7. Spatially targeted scenario analysis

The ability of the GRI model to estimate the impact of different measures is illustrated by running simple mitigation scenarios using 2016 data (baseline). According to the main pressures exerted on the studied aquifers (Table 3), and based on the results and discussion previously presented, two scenarios with spatially targeted measures (in addition to those in the ND/AP described in Appendix C), both preconizing a reduction in N loads were analysed.

i) Scenario LMA (low manure application)

This scenario considers a 50 % reduction on the maximum amount of manure that can be legally spread on the fields (170 kg N ha^{-1} is the current threshold). Scenario LMA is targeted for the central and southern part of the TVZ, where specialization has evolved towards livestock production, especially pigs, with livestock manure used to fertilize crops.

ii) Scenario LIC (low-input demanding crops)

This scenario considers measures targeted for the areas with very intensive irrigated agriculture, located in the north and western parts of the TVZ (Fig. 7). These areas present high and very high intrinsic vulnerabilities (Fig. 3) thus, the application of the ND/AP measures without changing the cropping patterns will probably not contribute to decrease the risk. Change from the annual irrigated maize and vegetable crops to more extensive forms of land use will decrease the N and irrigation inputs. Thus, the water and N surpluses were recalculated, considering the predominance of permanent grasslands and orchards in these areas. This corresponded to N surplus reductions between 25 and 75 kg ha^{-1}.

iii) Scenario LMA + LIC

In this scenario, GRI is predicted for the case when the two targeted measures are applied simultaneously. Municipality 7 is the only one with a superposition of the measures preconized in both scenarios.

Fig. 9 shows the Global Risk Index map for the baseline (real situation in 2016) and for the three scenarios. The results are only indicative of the effects of the measures. In general, the targeted measures produced positive results, decreasing the Risk Index to a low rate.

Scenario LMA produced reasonably good results for the central and southern TVZ territory, as it decreased the risk from very high to high and from high to Moderate in 11 % and 6% of the area, respectively. At the same time increase in 16 % the area with low risk to groundwater pollution. However, to implement this low manure application-based measure, additional measures are needed, including the increase in the manure storage capacity, so that farmers will be able to optimize manure application increasing the use efficiency. Also, the use of compost facilities to produce composts with high C/N and anaerobic digesters for the treatment of livestock excreta are proposed.

Scenario LIC also produced very good results since the high risk areas ended, the moderate risk areas decreased in 22 %, while the low risk areas increased in 55 %. Similar results were found by Tetzlaff et al. (2013) for the North Rhine-Westphalia (Germany) and Malagó et al. (2019) for the Mediterranean river basins. These authors showed that a 50 % decrease of nitrogen surplus on cropland and grass land in the Mediterranean river basins would entail more than 20 % reduction of nitrogen input to coastal waters. In the present study the exception was the strip of land parallel to the Tagus River in the northern part of TVZ, where the risk does not decrease below moderate. One possible reason is the high intrinsic vulnerability associated to nitrate residence times less than six months, due to the proximity of the Alluvial aquifer (in some places < 1 m). The other possible reason is related to a high specific vulnerability associated to the high aquifer recharge rates due to the intense autumn/winter precipitations typical of the Mediterranean climate. This percolating water rapidly washes the nitrates that stayed in the profile after the spring/summer crops harvest into the groundwater. However, scenario LIC is a very drastic and improbable one, since the intensive irrigated crops as maize and tomatoes for processing are the economical driver of the region. Nevertheless, it can provide a benchmark for the impact evaluation of mitigation measures.

Finally, by putting together the two types of measures (Scenario LMA + LIC) there is potential to end high risk areas, reduce moderate risk areas to 13 %, while the rest of the area will present a low risk to groundwater pollution.

4. Conclusions

An index-based methodology is presented to evaluate the impact of the EU Nitrates Directive (ND) and the Nacional Action Plans (AP) measures upon groundwater pollution with agricultural nitrates. Its originality lies in the fact that it incorporates two information layers defined with detailed municipality data: the N surplus, used to classify the N loading hazard and the water surplus were irrigation has an important role in the calculation of the aquifer recharges in Mediterranean zones. Its practical interest is illustrated for a Mediterranean nitrate vulnerable zone (NVZ).

Results show that though the study area has been under NVZ management since 2004–2010 and the N surplus shows an overall decrease, the groundwater quality status related to NO_3^- is not improving, but is aggravating instead. This confirms that the N surplus (or N balance), per se, is not a suitable agri-environmental indicator of the ND/AP measures effectiveness in improving the groundwater quality status. However, it constitutes a very important layer of the global pollution risk from agricultural activities as it incorporates in the model the effects of the

agricultural practices and their change over time.

The Global Risk Index model produced an indicator (GRI) for groundwater quality showing a reasonable consistency between the global risk associated to agricultural activity and groundwater pollution status at each point, despite model uncertainties. The GRI shows that different parts of the territory within the same NVZ, are exposed to different levels of N loading hazard and vulnerabilities influencing the risk of groundwater pollution with nitrates from agriculture activity. Thus, mitigation measures must be reformulated and spatially targeted according with both the N hazard and the aquifer vulnerability.

The GRI scenarios analysis showed that targeted measures addressing local specificities can be effective in decreasing the risk for groundwater pollution. Nevertheless, the important aquifer recharge associated to the intense autumn/winter precipitation that occur in the region, together with the very high intrinsic vulnerability (very low nitrate residence times) in some TVZ areas can be a constraint to further decrease the risk, independently of the N hazard reduction.

The method developed in this study offers a low-cost and relatively simple alternative to process based models, and/or expensive field experiments in screening areas where further detailed research is required for better understanding the relationship between N mitigation measures and groundwater nitrate levels. However, one possible improvement of the proposed model would be to considerate different factor weighting in the GRI index according to the aquifer type. Besides, access to a big dataset will allow the comparison with other empirical models and a better validation of results. Future work will focus on this.

Declaration of Competing Interest

The authors report no declarations of interest.

Acknowledgments

The authors acknowledge NitroPortugal, H2020-TWINN-2015, EU coordination and support action n. 692331 for funding. João Rolim was funded by FCT through the researcher contract DL 57/2016/CP1382/CT0021. LEAF (UID/AGR/04129/2019), CEF(UID/AGR/00239/2013) and CMAFcIO (UID/MAT/04561/2013) are research units funded by Fundação para a Ciência e a Tecnologia I.P. (FCT), Portugal.

Appendix A. Formulation of the water balance calculation at the municipality level

The water balance equation was applied independently to the irrigated and rainfed crop areas, assuming that for the latter $ETc = ET_0$ and $IRR = 0$. The WS for each municipality (WS_M) was calculated as a weighted average of the WS for the rainfed (WS_R) and the irrigated (WS_I) crop areas (Eq. A1):

$$WS_M = \frac{WS_R \times A_R + WS_I \times A_I}{AC_T} \quad (A1)$$

where A_R is the rainfed crop area (ha), A_I is the irrigated crop area (ha), and AC_T is the total crop area (ha) in the municipality.

For the irrigated areas, crop evapotranspiration (ETc) was estimated according to the crop coefficient (Kc) methodology (Eq. A2, Allen et al., 1998):

$$ETc = Kc_M \times ETo \quad (A2)$$

where ETc is the crop evapotranspiration (mm month^{-1}), Kc_M is the monthly crop coefficient (dim) and ETo is the reference evapotranspiration (mm month^{-1}).

The Hargreaves-Samani equation (Hargreaves and Samani, 1985) which requires temperature data only was used (Eq. A3), since the complete set of meteorological variables necessary for the calculation of ETo according to the FAO Penman-Monteith (Allen et al., 1998) method was not available.

$$ET_o = \alpha(T + 17.78)(T_{max} - T_{min})^{0.5} R_a \quad (A3)$$

where $\alpha = 0.0023$, T_{max} and T_{min} are the maximum and minimum air temperatures (^oC), respectively, and R_a is the extra-terrestrial radiation (MJ m^{-2} d^{-1}).

The K_c curves were built for each crop from the specific coefficient values for the different stages extracted from FAO 56 (Allen et al., 1998). The monthly K_c values extracted from those curves were weighted by the areas occupied by each crop, producing an average monthly K_{cM} for each municipality and period, according to Eq. A4:

$$Kc_M = \frac{\sum_{i=1}^{n} AC_i \times Kc_i}{AC_T} \quad (A4)$$

where AC_i is the area occupied by the crop i (ha), Kc_i is the crop coefficient for crop i (dim) and AC_T is the total area (ha) occupied by the n crops in the municipality.

Finally, the irrigation depths for the entire study period were calculated using the net irrigation amounts (IN_M, Eq. A5) and average irrigation efficiencies for each municipality and period (EF, Eq. 6).

$$IN_M = \frac{\sum_{i=1}^{n} AC_i\ IN_i}{AC_T} \quad (A5)$$

where IN_i is the net irrigation requirement for crop i (mm), and n is the number of crops in the municipality.

$$EF = \frac{\sum_{i=1}^{n} AC_i\ .\ EF_i}{AC_T} \quad (A6)$$

where EF_i is the irrigation efficiency for crop i (fraction).

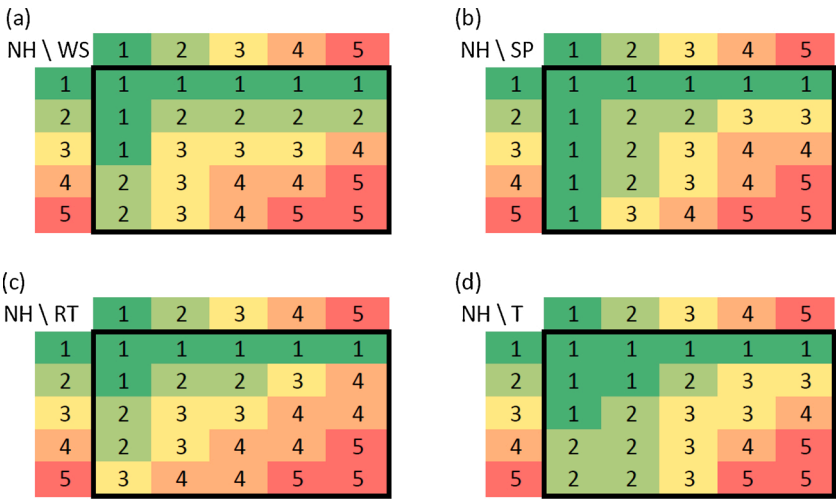

Fig. A1. Rule-based approach for the calculation of the indices $I_{NH\times WS}$ (a), $I_{NH\times SP}$ (b), $I_{NH\times RT}$ (c) and $I_{NH\times T}$ (d).

Appendix B. Rule-based approach to the four indexes, components of GRI

.

Appendix C. The Tagus Vulnerable Zone and the National Action Plan

The initially designated TVZ area (Ordinance 1100/2004) comprised 19,000 ha but was subsequently extended (Ordinance 1433/2006) to 100,000 ha. A further extension (Ordinance 1366/2010) increased the TVZ to the current 241,686 ha.

The compulsory measures presented in the Portuguese National Action Plan (ND/AP) regarding crops' fertilization are (1) the correction of the amount of mineral N applied to crops by deducting in the fertilization requirements the N entering via irrigation water and the N provided by the crop residues left in the field after the harvest of previous crops; (2) The limitation of the amount of manure applications to the crops to 170 kg N ha^{-1} yr^{-1}; (3) the limitation of the total N (mineral + organic) applications to the crops as described in the National Action Plan.

Appendix D. Supplementary data

Supplementary material related to this article can be found, in the online version, at doi:https://doi.org/10.1016/j.agee.2020.107204.

References

Ahuja, L., Rojas, K.W., Hanson, J.D., 2000. Root Zone Water Quality Model: Modelling Management Effects on Water Quality and Crop Production. Water Resources Publication, USA, p. 373.

Allen, R.G., Pereira, L.S., Raes, D., Smith, M., 1998. Crop evapotranspiration. Guidelines for computing crop water requirements. FAO Irrigation and Drainage Paper 56. FAO, Rome, Italy, p. 300.

Aller, L., Bennett, T., Lehr, J.H., Petty, R.J., 1985. Drastic: a Standardized System for Evaluating Groundwater Pollution Potential Using Hydrogeologic Settings. EPA/600/2-85/018 U.S. Environmental Protection Agency, Robert S. Kerr Environmental Research Laboratory, Office of Research and Development.

Almeida, C., Mendonça, J.L., Jesus, M.R., Gomes, A.J., 2000. Sistemas Aquíferos De Portugal Continental, Relatório INAG. Instituto da Água, Lisboa (2000) Electr. Doc., CD-ROM (in Portuguese).

APA, 2016. Plano De Gestão Das Regiões Hidrográficas. Região hidrográfica do Tejo e Ribeiras do oeste (RH5), Lisboa (in Portuguese).

Arauzo, M., 2017. Vulnerability of groundwater resources to nitrate pollution: a simple and effective procedure for delimiting Nitrate Vulnerable Zones. Sci. Total Environ. 575, 799–812. https://doi.org/10.1016/j.scitotenv.2016.09.139.

Arauzo, M., Martínez-Bastida, J.J., 2015. Environmental factors affecting diffuse nitrate pollution in the major aquifers of central Spain: groundwater vulnerability vs. Groundwater pollution. Environ. Earth Sci. 73 (12), 8271–8286. https://doi.org/10.1007/s12665-014-3989-8.

Arauzo, M., Valladolid, M., 2013. Drainage and N-leaching in alluvial soils under agricultural land uses: implications for the implementation of the EU Nitrates Directive. Agric. Ecosyst. Environ. 179, 94–107. https://doi.org/10.1016/j.agee.2013.07.013.

Arauzo, M., Valladolid, M., Martínez-Bastida, J.J., 2011. Spatio-temporal dynamics of nitrogen in river-alluvial aquifer systems affected by diffuse pollution from agricultural sources: implications for the implementation of the Nitrates Directive. J. Hydrol. (Amst) 411 (1-2), 155–168.

Arnold, J.G., Moriasi, D.N., Gassman, P.W., Abbaspour, K.C., White, M.J., Srinivasan, R., Santhi, C., Harmel, D., van Griensven, A., Liew, Van, Michael, W., Kannan, N., Jha, M., 2012. SWAT: model use, calibration, and validation. TASABE 55 (4), 1491–1508.

Ascott, M.J., Gooddy, D.C., Wang, L., Stuart, M.E., Lewis, M.A., Ward, R.S., Binley, A.M., 2017. Global patterns of nitrate storage in the vadose zone. Nat. Commun. 8 (1), 1416.

Baily, A., Rock, L., Watson, C.J., Fenton, O., 2011. Spatial and temporal variations in groundwater nitrate at an intensive dairy farm in south-east Ireland: insights from stable isotope data. Agric. Ecosyst. Environ. 144 (1), 308–318. https://doi.org/10.1016/j.agee.2011.09.007.

Bartels, R., 1982. The rank version of von Neumann's ratio test for randomness. J. Am. Stat. Assoc. 77 (377), 40–46.

Bouraoui, F., Grizzetti, B., Aloe, A., 2011. Long term nutrient loads entering European seas. European Commission, Luxembourg 72.

Boyd, S., Vandenberghe, L., 2004. Convex Optimization. Cambridge University Press.

Boy-Roura, M., Nolan, B.T., Menció, A., Mas-Pla, J., 2013. Regression model for aquifer vulnerability assessment of nitrate pollution in the Osona región (NE Spain). J. Hydrol. (Amst) 505, 150–162. https://doi.org/10.1016/j.jhydrol.2013.09.048.

Brindha, K., Elango, L., 2013. Causes for variation in bromide concentration in groundwater of a granitic aquifer. Int J Res Chem Environ 3 (2), 163–171.

Buczko, U., Kuchenbuch, R.O., 2010. Environmental indicators to assess the risk of diffuse nitrogen losses from agriculture. Environmental Manag. 45 (5), 1201–1222. https://doi.org/10.1007/s00267-010-9448-8.

Cameira, M.R., Pereira, A., Ahuja, L., Ma, L., 2014. Sustainability and environmental assessment of fertigation in an intensive olive grove under Mediterranean conditions. Agr. Water Manage. 146, 346–360. https://doi.org/10.1016/j.agwat.2014.09.007.

Cameira, M.R., Rolim, J., Valente, F., Faro, A., Dragosits, U., Cordovil, C.M., 2019. Spatial distribution and uncertainties of nitrogen budgets for agriculture in the Tagus river basin in Portugal–Implications for effectiveness of mitigation measures. Land Use Policy 84, 278–293. https://doi.org/10.1016/j.landusepol.2019.02.028.

Cardoso, J.C., 1965. Os solos de Portugal, sua classificação, caracterização e génese. 1 –A sul do rio tejo. Ministério da Agricultura, Lisboa (in portuguese).

Cardoso, R.M., Soares, P.M.M., Lima, D.C.A., Miranda, P.M.A., 2019. Mean and extreme temperatures in a warming climate: EURO CORDEX and WRF regional climate high-resolution projections for Portugal. Clim. Dyn. 52, 129–157. https://doi.org/10.1007/s00382-018-4124-4.

Civita, M., De Maio, M., 1997. SINTACS – Un sistema parametrico per la valutazione e la cartografia della vulnerabilità degli acquiferi all''nquinamento. Quaderni di tecniche di protezione ambientale, Pitagora Editrice, Bologna n. 60.
Cordovil, C., Cruz, S., Brito, A., Cameira, M., Poulsen, J., Thodsen, H., Kronvang, B., 2018. A simplified nitrogen assessment in Tagus River Basin: a management focused review. Water 10 (4), 406. https://doi.org/10.3390/w10040406.
Cruz, S., Cordovil, C.M., Pinto, R., G Brito, A., Cameira, M.R., Gonçalves, G., Poulsen, J. R., Thodsen, H., Kronvang, B., May, L., 2019. Nitrogen in water-Portugal and Denmark: two contrasting realities. Water 11 (6), 1114. https://doi.org/10.3390/w11061114.
Da Cunha, L.V., De Oliveira, R.P., Nascimento, J., Ribeiro, L., 2007. Impacts of Climate Change on Water Resources: a Case-Study for Portugal, 310. IAHS publication, p. 37.
De Ruijter, F.J., Boumans, L.J.M., Smit, A.L., Van den Berg, M., 2007. Nitrate in upper groundwater on farms under tillage as affected by fertilizer use, soil type and groundwater table. *Nutr.* Cycling in Agroecosystems 77 (2), 155–167. https://doi.org/10.1007/s10705-006-9051-9.
Debernardi, L., De Luca, D.A., Lasagna, M., 2008. Correlation between nitrate concentration in groundwater and parameters affecting aquifer intrinsic vulnerability. Environ. Geol. 55 (3), 539–558. https://doi.org/10.1007/s00254-007-1006-1.
Erisman, J.W., Galloway, J.N., Seitzinger, S., Bleeker, A., Dise, N.B., Petrescu, A.R., Leach, A.M., de Vries, W., 2013. Consequences of human modification of the global nitrogen cycle. Philos. Trans. Biol. Sci. 368 (1621), 20130116. https://doi.org/10.1098/rstb.2013.0116.
Eurostat, 2016. Agriculture, forestry and fishery statistics. European Union. Eurostat/OECD.2013 Nutrient Budgets Methodology and Handbook.
Foster, S.S.D., Witkowski, A.J., Kowalczyk, A., Vrba, J., 2007. Aquifer pollution vulnerability concept and tools—use, benefits and constraints. Groundwater vulnerability assessment and mapping. IAH-selected Papers 11, 2–9.
Foster, S., Hirata, R., Andreo, B., 2013. The aquifer pollution vulnerability concept: aid or impediment in promoting groundwater protection? Hydrogeol. J. 21 (7), 1389–1392. https://doi.org/10.1007/s10040-013-1019-7.
Giorgi, F., Lionello, P., 2008. Climate change projections for the Mediterranean region. Global Planet Change 63, 90–104. https://doi.org/10.1016/j.gloplacha.2007.09.005.
Grizzetti, B., Bouraoui, F., De Marsily, G., 2008. Assessing nitrogen pressures on European surface water. Global Biogeochem. Cycles 22 (4).
Hagedorn, B., Clarke, N., Ruane, M., Faulkner, K., 2018. Assessing aquifer vulnerability from lumped parameter modeling of modern water proportions in groundwater mixtures: application to California's south Coast Range. Sci. Total Environ. 624, 1550–1560. https://doi.org/10.1016/j.scitotenv.2017.12.115.
Hansen, B., Dalgaard, T., Thorling, L., Sørensen, B., Erlandsen, M., 2012. Regional analysis of groundwater nitrate concentrations and trends in Denmark in regard to agricultural influence. Biogeosciences Discuss. 9 (5) https://doi.org/10.5194/bg-9-3277-2012.
Hargreaves, G.H., Samani, Z.A., 1985. Reference crop evapotranspiration from temperature. Appl. Eng. Agric. 1 (2), 96–99. https://doi.org/10.13031/2013.26773.
Hettmansperger, T.P., McKean, J.W., Sheather, S.J., 1997. 7 Rank-based analyses of linear models. Handbook of statistics 15, 145–173.
Holman, I.P., Palmer, R.C., Bellamy, P.H., Hollis, J.M., 2005. Validation of an intrinsic groundwater pollution vulnerability methodology using a national nitrate database. Hydrogeol. J. 13 (5-6), 665–674. https://doi.org/10.1007/s10040-005-0439-4.
IBM, 2017. IBM ILOG CPLEX Optimization Studio V12.8.0. www.cplex.com.
Iuss Working Group Wrb, 2015. World reference base for soil resources 2014, update 2015: International soil classification system for naming soils and creating legends for soil maps. World Soil Resources Reports No. 106, p. 192.
Kasper, M., Foldal, C., Kitzler, B., Haas, E., Strauss, P., Eder, A., Zechmeister-Boltenstern, S., Amon, B., 2019. N_2O emissions and NO_3− leaching from two contrasting regions in Austria and influence of soil, crops and climate: a modelling approach. Nutr. Cycling Agroecosyst. 113 (1), 95–111. https://doi.org/10.1007/s10705-018-9965-z.
Kazakis, N., Voudouris, K.S., 2015. Groundwater vulnerability and pollution risk assessment of porous aquifers to nitrate: modifying the DRASTIC method using quantitative parameters. J. Hydrol. (Amst) 525, 13–25. https://doi.org/10.1016/j.jhydrol.2015.03.035.
Keuskamp, J.A., Van Drecht, G., Bouwman, A.F., 2012. European-scale modelling of groundwater denitrification and associated N2O production. Environ. Pollut. 165, 67–76. https://doi.org/10.1016/j.envpol.2012.02.008.
Kilsby, C.G., Tellier, S.S., Fowler, H.J., Howels, T.R., 2007. Hydrological impacts of climate change on the Tejo and Guadiana Rivers. Hydrol. Earth Syst. Sci. Discuss. 11 (3), 1175–1189.
Kim, H.R., Yu, S., Oh, J., Kim, K.H., Lee, J.H., Moniruzzaman, M., Kim, H.K., Yun, S.T., 2019. Nitrate contaminationpollution and subsequent hydrogeochemical processes of shallow groundwater in agro-livestock farming districts in South Korea. Agric. Ecosyst. Environ. 273, 50–61. https://doi.org/10.1016/j.agee.2018.12.010.
Komsta, L., 2019. mblm: Median-Based Linear Models. R package version 0.12.1. https://CRAN.R-project.org/package=mblm.
Kovats, R.S., Valentini, R., Bouwer, L.M., Georgopoulou, E., Jacob, D., Martin, E., Rounsevell, M., Soussana, J.-F., 2014. Europe. In: Barros, V.R., Field, C.B., Dokken, D.J., Mastrandrea, M.D., Mach, K.J., Bilir, T.E., Chatterjee, M., Ebi, K.L., Estrada, Y.O., Genova, R.C., Girma, B., Kissel, E.S., Levy, A.N., MacCracken, S., Mastrandrea, P.R., White, L.L. (Eds.), Climate Change 2014: Impacts, Adaptation, and Vulnerability. Part B: Regional Aspects. Contribution of Working Group II to the Fifth Assessment Report of the Intergovernmental Panel on Climate Change. Cambridge University Press, Cambridge, United Kingdom and New York, NY, USA, pp. 1267–1326.
Lassaletta, L., Romero, E., Billen, G., Garnier, J., García-Gómez, H., Rovira, J.V., 2012. Spatialized N budgets in a large agricultural Mediterranean watershed: high loading and low transfer. Biogeosciences 9 (1), 57–70. https://doi.org/10.5194/bg-9-57-2012 https://doi.org/10.5194/bg-9-57-2012.
Leone, A., Ripa, M.N., Uricchio, V., Dea, J., Vargay, Z., 2009. Vulnerability and risk evaluation of agricultural nitrogen pollution for Hungary's main aquifer using DRASTIC and GLEAMS models. J. Environ. Manag. 90, 2969–2978. https://doi.org/10.1016/j.jenvman.2007.08.009.
Li, Z., Wen, X., Hu, C., Li, X., Li, S., Zhang, X., Hu, B., 2020. Regional simulation of nitrate leaching potential from winter wheat-summer maize rotation croplands on the North China Plain using the NLEAP-GIS model. Agric. Ecosyst. Environ. 294, 106861. https://doi.org/10.1016/j.agee.2020.106861.
Lord, E.I., Anthony, S.G., Goodlass, G., 2002. Agricultural nitrogen balance and water quality in the UK. Soil Use Manag. 18 (4), 363–369. https://doi.org/10.1111/j.1475-2743.2002.tb00253.x.
Malagó, A., Bouraoui, F., Vigiak, O., Grizzetti, B., Pastori, M., 2017. Modelling water and nutrient fluxes in the Danube River Basin with SWAT. Sci. Total Environ. 603, 196–218. https://doi.org/10.1016/j.scitotenv.2017.05.242.
Malagó, A., Bouraoui, F., Grizzetti, B., De Roo, A., 2019. Modelling nutrient fluxes into the Mediterranean Sea. J. Hydrol.: Regional Studies 22, 100592.
Martínez-Bastida, J.J., Arauzo, M., Valladolid, M., 2010. Intrinsic and specific vulnerability of groundwater in central Spain: the risk of nitrate pollution. Hydrogeol. J. 18 (3), 681–698. https://doi.org/10.1007/s10040-009-0549-5.
Mateus, A., Caeiro, F., 2014. An R implementation of several randomness tests. In: American Institute of PhysicsAIP Conference Proceedings, 1618, pp. 531–534 (1).
Mendes, M.P., Ribeiro, L., 2010. Nitrate probability mapping in the northern aquifer alluvial system of the river Tagus (Portugal) using Disjunctive Kriging. Sci. Total Environ. 408 (5), 1021–1034. https://doi.org/10.1016/j.scitotenv.2009.10.069.
Mendonça, J.J.L., 1996. Características hidráulicas do aquífero terciário do Tejo e do Sado na região de Vila Franca de Xira. Recursos Hídricos 17 (2), 53–66 e 3 (in Portuguese).
Mendonça, J.J.L., 2009. Caraterização geológica e hidrogeológica da Bacia Terciária do Tejo-Sado. Administração da Região Hidrográfica do Tejo IP, Tagides: Os Aquíferos das Bacias Hidrográficas do Rio Tejo e das Ribeiras do Oeste-Saberes e Reflexões, pp. 59–66.
Meng, L., Zhang, Q., Liu, P., He, H., Xu, W., 2020. Influence of agricultural irrigation activity on the potential risk of groundwater pollution: a study with drastic method in a semi-arid agricultural region of China. Sustainability 12 (5), 1954.
Molina-Herrera, S., Haas, E., Klatt, S., Kraus, D., Augustin, J., Magliulo, V., Tallec, T., Ceschia, E., Ammann, C., Loubet, B., Skiba, U., Jones, S., Brümmer, C., Butterbach-Bahl, K., Kiese, R., 2016. A modeling study on mitigation of N2O emissions and NO3 leaching at different agricultural sites across Europe using Landscape DNDC. Sci. Total Environ. 553, 128–140. https://doi.org/10.1016/j.scitotenv.2015.12.099.
Nolan, B.T., Gronberg, J.M., Faunt, C.C., Eberts, S.M., Belitz, K., 2014. Modeling nitrate at domestic and public-supply well depths in the Central Valley. California. Environ. Sci. Technol. 48 (10), 5643–5651. https://doi.org/10.1021/es405452q.
Nolan, B.T., Fienen, M.N., Lorenz, D.L., 2015. A statistical learning framework for ground-water nitrate models. J. Hydrol. (Amst) 531, 902–911. https://doi.org/10.1016/j.jhydrol.2015.10.025.
Pacheco, F.A.L., Pires, L.M.G.R., Santos, R.M.B., Fernandes, L.S., 2015. Factor weighting in DRASTIC modeling. Sci. Total Environ. 505, 474–486. https://doi.org/10.1016/j.scitotenv.2014.09.092.
Pires, V., Cota, T.M., Silva, A., 2018. Alterações observadas no clima atual e cenários climáticos em Portugal continental – Influência no setor agrícola. Cultivar- Cadernos de Análise e Prospetiva. GPP, Portugal, pp. 57–67.
Pisciotta, A., Cusimano, G., Favara, R., 2015. Groundwater nitrate risk assessment using intrinsic vulnerability methods: a comparative study of environmental impact by intensive farming in the Mediterranean region of Sicily, Italy. J. Geochem. Explor. 156, 89–100. https://doi.org/10.1016/j.gexplo.2015.05.002.
R Core Team, 2018. R: a Language and Environment for Statistical Computing. URL. R Foundation for Statistical Computing, Vienna, Austria. https://www.R-project.org/.
R Studio Team, 2018. RStudio: Integrated Development for R. RStudio, Inc, Boston, MA.
Refsgaard, J.C., Thorsen, M., Jensen, J.B., Kleeschulte, S., Hansen, S., 1999. Large scale modeling of groundwater contaminationpollution from nitrate leaching. J. Hydrol. (Amst) 221, 117–140. https://doi.org/10.1016/S0022-1694(99)00081-5.
Rivett, M.O., Buss, S.R., Morgan, P., Smith, J.W., Bemment, C.D., 2008. Nitrate attenuation in groundwater: a review of biogeochemical controlling processes. Water Res. 42 (16), 4215–4232. https://doi.org/10.1016/j.watres.2008.07.020.
Rizeei, H.M., Azeez, O.S., Pradhan, B., Khamees, H.H., 2018. Assessment of groundwater nitrate contamination hazard in a semi-arid region by using integrated parametric IPNOA and data-driven logistic regression models. Environ. Monit. Assess. 190 (11), 633.
Rodriguez-Galiano, V., Mendes, M.P., Garcia-Soldado, M.J., Chica-Olmo, M., Ribeiro, L., 2014. Predictive modeling of groundwater nitrate pollution using Random Forest and multisource variables related to intrinsic and specific vulnerability: a case study in an agricultural setting (Southern Spain). Sci. Total Environ. 476–477, 189–206. https://doi.org/10.1016/j.scitotenv.2014.01.001.
Rolim, J., Catalão, J., Teixeira, J.L., 2011. The influence of different methods of interpolating spatial meteorological data on calculated irrigation requirements. Appl. Eng. Agric. 27 (6), 979–989. https://doi.org/10.13031/2013.40625.
Rolim, J., Navarro, A., Vilar, P., Saraiva, C., Catalão, J., 2019. Crop data retrieval using earth observation data to support agricultural water management. Eng. Agrã¯â¿â½cola 39 (3), 380–390. https://doi.org/10.1590/1809-4430.
Rotiroti, M., Bonomi, T., Sacchi, E., McArthur, J.M., Stefania, G.A., Zanotti, C., Taviania, S., Patellia, M., Navaa, V., Solera, V., Fumagalli, L., 2019. The effects of irrigation on groundwater quality and quantity in a human-modified hydro-system:

the Oglio River basin, Po Plain, northern Italy. Sci. Total Environ. 672, 342–356. https://doi.org/10.1016/j.scitotenv.2019.03.427.
Salman, S.A., Arauzo, M., Elnazer, A.A., 2019. Groundwater quality and vulnerability assessment in west Luxor Governorate, Egypt. Groundw. Sustain. Dev. 8, 271–280. https://doi.org/10.1016/j.gsd.2018.11.009.
Sen, P.K., 1968. Estimates of the regression coefficient based on Kendall's tau. J. Am. Stat. Assoc. 63 (324), 1379–1389.
Serra, J., Cordovil, C.M., Cruz, S., Cameira, M.R., Hutchings, N.J., 2019. Challenges and solutions in identifying agricultural pollution hotspots using gross nitrogen balances. Agric. Ecosyst. Environ. 283, 106568 https://doi.org/10.1016/j.agee.2019.106568.
Shahidian, S., Teixeira, J.L., Serrano, J., Rolim, J., 2014. Estudo comparativo das alterações climáticas e da sua influência sobre as necessidades de rega no clima mediterrâneo (comparative study of climate change and its influence on irrigation requirements in the Mediterranean climate). "VII Congresso ibérico de agroingenieria y ciências hortícolas: Innovar y producir para el futuro". Fundación General de la Universidad Politécnica de Madrid ed., Madrid, Espanha, pp. 555–560.
Sieling, K., Kage, H., 2006. N balance as an indicator of N leaching in an oilseed rape–winter wheat–winter barley rotation. Agric. Ecosyst. Environ. 115 (1-4), 261–269.
Soares, P.M.M., Cardoso, R.M., Lima, D.C.A., Miranda, P.M.A., 2017. Future precipitation in Portugal: high-resolution projections using WRF model and EURO-CORDEX multi-model ensembles. Clim. Dyn. 49, 2503–2530. https://doi.org/10.1007/s00382-016-3455-2.
Sousa, P.L., Morais, A., 2011. MECAR: metodologia para a estimativa de água de rega em Portugal. In: Sousa, P.L., Ribeiro, L. (Eds.), O Uso Da água Na Agricultura. INE, Lisboa (in Portuguese).
Stigter, T.Y., Ribeiro, L., Dill, A.C., 2006. Evaluation of an intrinsic and a specific vulnerability assessment method in comparison with groundwater salinisation and nitrate contamination levels in two agricultural regions in the south of Portugal. Hydrogeol. J. 14 (1-2), 79–99. https://doi.org/10.1007/s10040-004-0396-3.
Stigter, T.Y., Nunes, J.P., Pisani, B., Fakir, Y., Hugman, R., Li, Y., Tomé, S., Ribeiro, L., Samper, J., Oliveira, R., Monteiro, J.P., Silva, A., Tavares, P.C.F., Shapouri, M., Cancela da Fonseca, L., Yacoubi-Khebiza, M., El Himer, H., 2014. Comparative assessment of climate change impacts on coastal groundwater resources and dependent ecosystems in the Mediterranean. Reg. Environ. Chang. 14 (Suppl 1), 41–56.
Sutton, M.A., Howard, C.M., Erisman, J.W., Billen, G., Bleeker, A., Grennfelt, P., Van Grinsven, H., Grizzetti, B. (Eds.), 2011. The European Nitrogen Assessment: Sources, Effects and Policy Perspectives. Cambridge University Press.
Tetzlaff, B., Kreins, P., Kuhr, P., Kunkel, R., Wendland, F., 2013. Grid-based modelling of nutrient inputs from diffuse and point sources for the state of North Rhine-Westphalia (Germany) as a tool for river basin management according to EU-WFD. River Syst. 20 (3-4), 213–229. https://doi.org/10.1127/1868-5749/2013/0060.
Thiel, H., 1950. A rank-invariant method of linear and polynomial regression analysis, part 3. Proceedings of Koninalijke Nederlandse Akademie Van Weinenschatpen A Volume 53, 1397–1412.
Uricchio, V.F., Giordano, R., Lopez, N., 2004. A fuzzy knowledge-based decision support system for groundwater pollution risk evaluation. J. Environ. Manag. 73 (3), 189–197. https://doi.org/10.1016/j.jenvman.2004.06.011.
van Beynen, P.E., Niedzielski, M.A., Bialkowska-Jelinska, E., Alsharif, K., Matusick, J., 2012. Comparative study of specific groundwater vulnerability of a karst aquifer in central Florida. Appl. Geogr. 32 (2), 868–877. https://doi.org/10.1016/j.apgeog.2011.09.
Van Grinsven, H.J.M., Ten Berge, H.F.M., Dalgaard, T., Fraters, B., Durand, P., Hart, A., Hofman, G., Jacobsen, B.H., Lalor, S.T., Lesschen, J.P., Osterburg, B., 2012. Management, regulation and environmental impacts of nitrogen fertilization in northwestern Europe under the Nitrates Directive: a benchmark study. Biogeosciences. 9 (12), 5143–5160. https://doi.org/10.5194/bg-9-5143-2012.
Vogelbacher, A., Kazakis, N., Voudouris, K., Bold, S., 2019. Groundwater vulnerability and risk assessment in a karst aquifer of Greece using EPIK method. Environments 6 (11), 116.
Vrba, J., Zaporozec, A., 1994. Guidebook on mapping groundwater vulnerability. 16. IAH Internationnal Contributions to Hydrogeology. Heise, p. 156.
Wang, H., Jiang, X.W., Wan, L., Han, G., Guo, H., 2015. Hydrogeochemical characterization of groundwater flow systems in the discharge area of a river basin. J. Hydrol. (Amst) 527, 433–441. https://doi.org/10.1016/j.jhydrol.2015.04.063.

Web References

CLC, 2018. https://land.copernicus.eu/pan-european/corine-land-cover/clc2018. (assessed in March 2020).

DGT- Direção-Geral do Território. http://www.dgterritorio.pt (accessed in January 2018).

ECA&D- European Climate Assessment & Dataset project. https://www.ecad.eu (accessed, June 2018).

EEA. 2018. https://www.eea.europa.eu/data-and-maps/indicators/agriculture-nitrogen-balance (accessed in July 2018).

Golden Software. https://www.goldensoftware.com/products/surfer.

INE - Instituto Nacional de Estatística. https://www.ine.pt. (accessed in June 2019).

SNIAmb - Sistema Nacional de Informação de Ambiente. https://sniamb.apambiente.pt/ (accessed in January 2019).

SNIRH - Sistema Nacional de Informação de Recursos Hídricos. https://snirh.apambiente.pt/. (accessed in August 2019).

USDA. United States Department of Agriculture: National Soil Survey Handbook (NSSH). 1983. http://www.nrcs.usda.gov/wps/portal/nrcs/detail/national/soils/?cid=nrcs142p2_054242. (accessed in December 2018).